PET Basics - Nuclear Medicine Multi Modality Imaging

Mika Teräs

Chief Physicist, Dep of Medical Physics, TUH
Professor, Institute of Biomedicine, UTU

Turku PET Centre

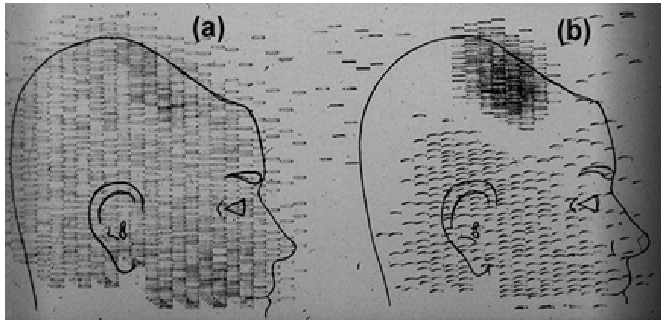

Figure 2: Coincidence and unbalance scans of patient with recurring brain tumor. Coincidence scan (a) of a patient showing recurrence of tumor under previous operation site, and unbalance scan (b) showing asymmetry to the left. (Reproduced from Brownell and Sweet 1953 [8]).

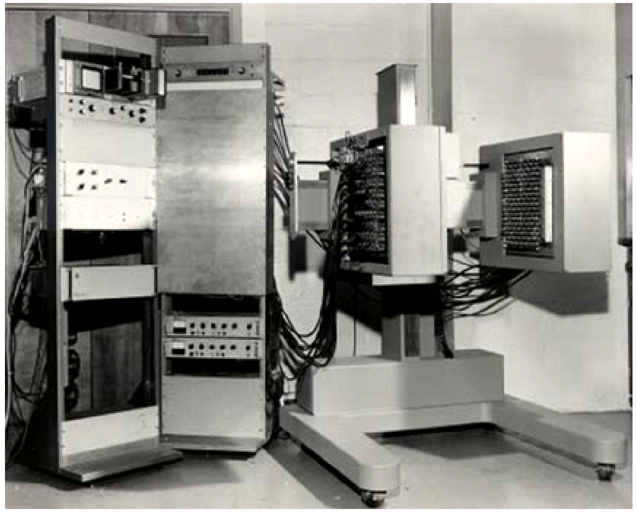

PC-I, the first tomographic PET

BROWNELL et al.
``Quantitative dynamic studies using short-lived radioisotopes and positron detection" in *Proceedings of the Symposium on Dynamic Studies with Radioisotopes in Medicine*, Rotterdam. August 31 - September 4, 1970. IAEA. **Vienna. 1971. pp. 161-172**.

Astro-Medical Imaging
Turku 21.5.2018

Quantitative Imaging Biomarkers Alliance

Entire chain of process determines quantitative result of an imaging biomaker

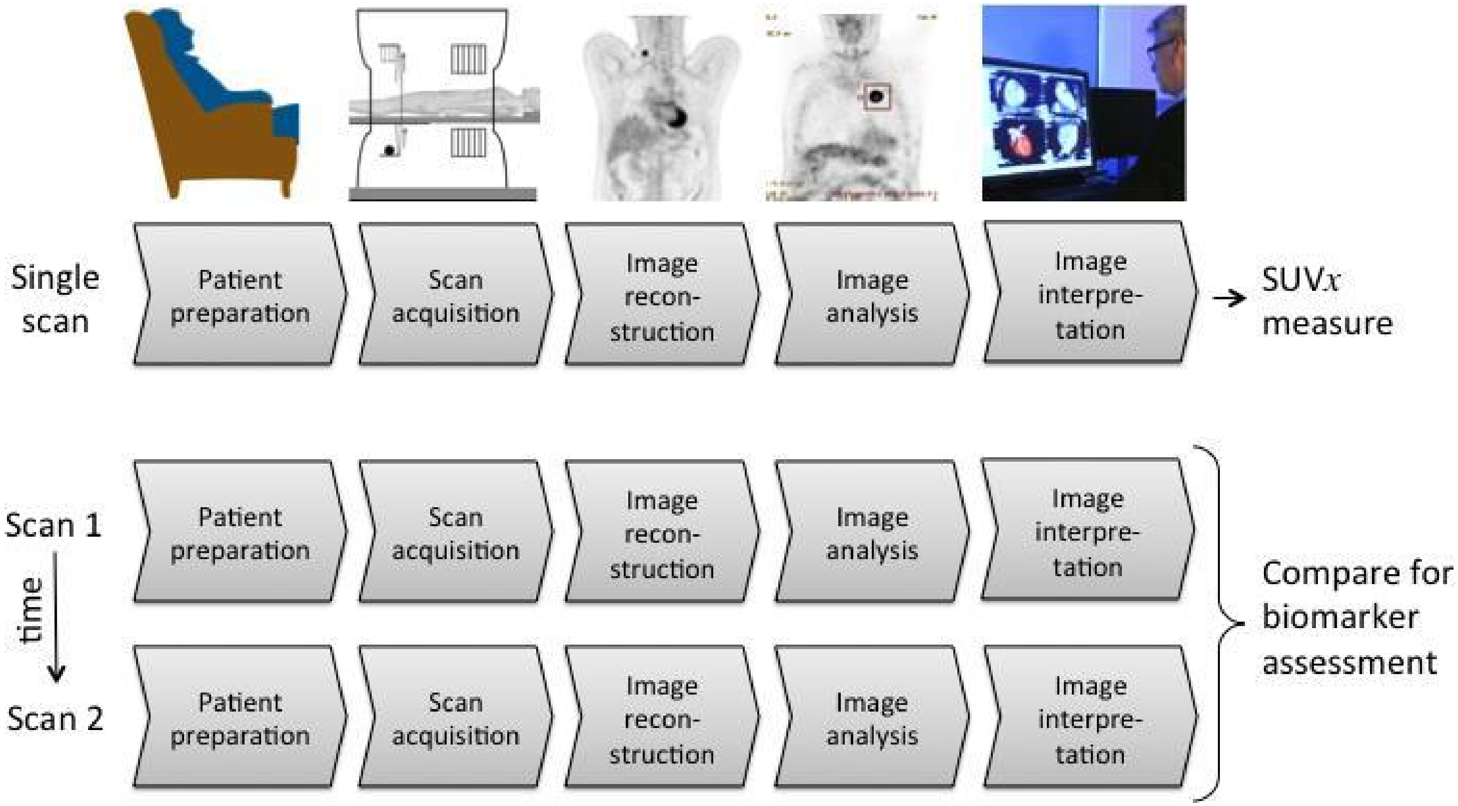

Picture taken from QIBA FDG PET/CT profile (www.**RSNA.ORG/QIBA**)

The role of medical imaging modalities

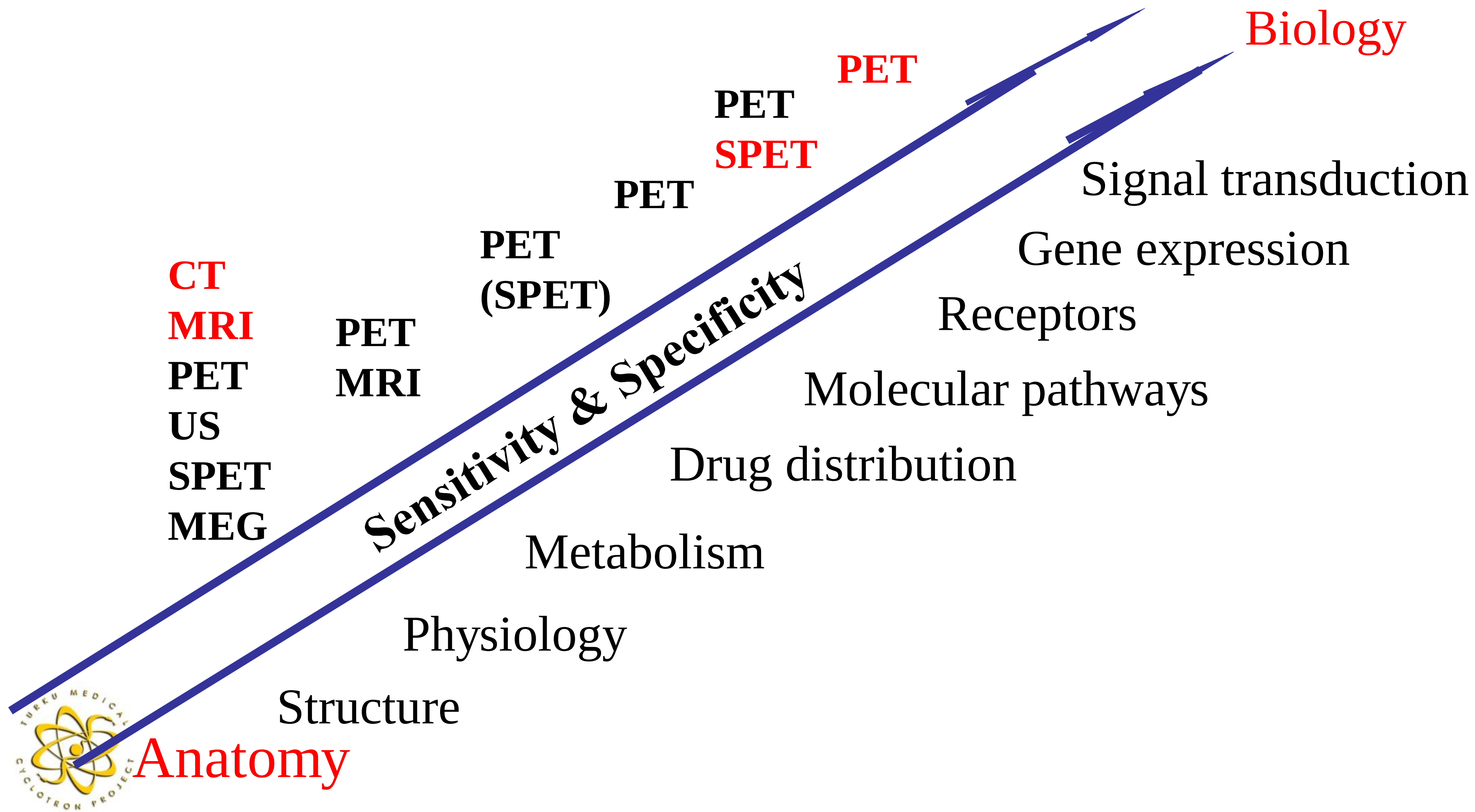

Why Multimodality?

Some benefits

- Better anatomical definition of (S)PET for reading
- Precise attenuation correction (AC) for quantification
- Anatomy based Partial Volume correction (PVC)
- New motion correction (MoCo) algorithms

History of MMMI

1989 1992 1995 1998 1999 2000 2010

Software

Commercial PET/CT systems

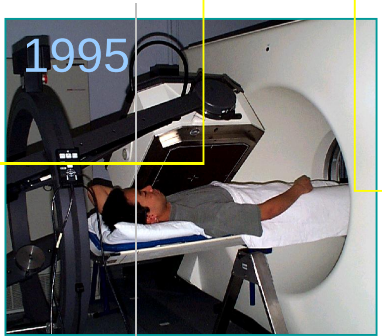

Hasegawa (UCSF) CT/SPECT

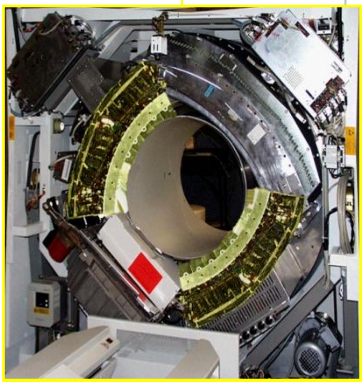

Townsend (UPMC) PET/CT

MR-PET 2011

PET-based hybrid imaging

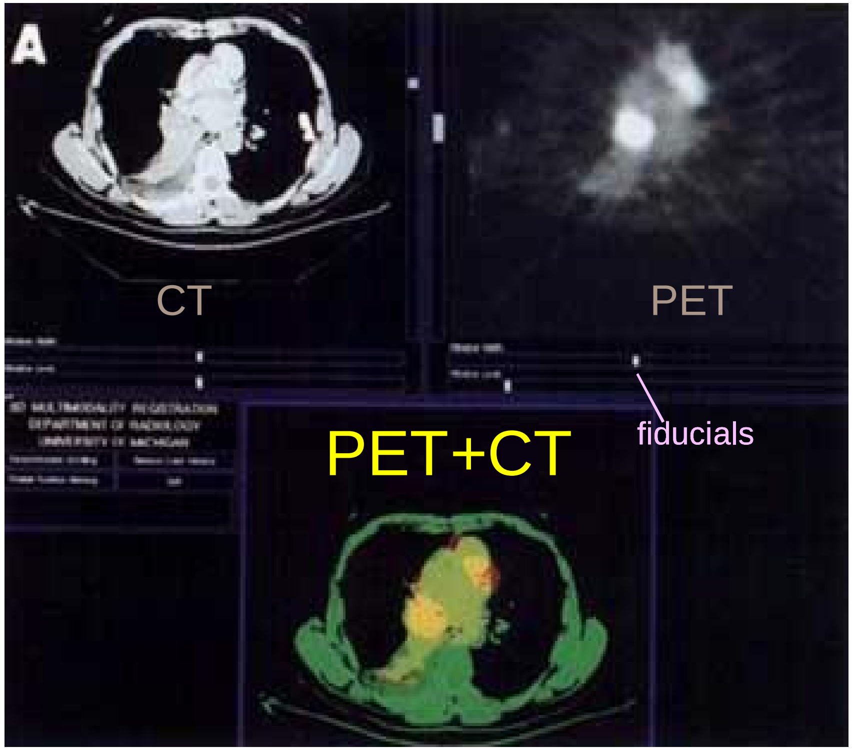

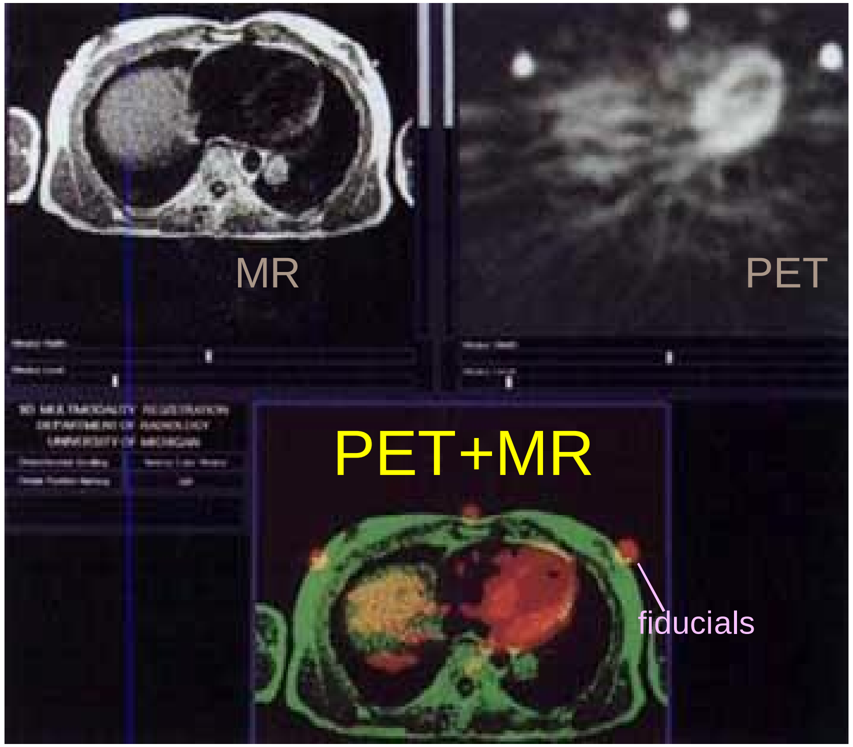

"… Anatometabolic fusion images made using this reasonably simple method [external fiducial landmarks] should prove useful in the management of patients with cancer and other diseases. …"
Wahl R et al, JNM 34, 1993

Anato-metabolic imaging = Complementary imaging

Physics - Identification

- Detection (up to 511 keV)
  - Detector properties
  - Electronics (speed, data handling)
- Imaging
  - Choice of modality
    - availability
    - Patient dose, ALARA
  - Choice of biomarker
  - Imaging protocol (patient preparation)
- Image reconstruction
  - Algorithms
  - Corrections (psf→ PV, motion)
- Modelling
  - Quantification
  - Signalling
  - Uncertainty analysis
- Standardisation
  - National
  - Global
- Big Data
  - National PACS
  - Bio banks
  - Reference databases
  - Automated analysis

Single Photon Emission Tomography SPET with CT

Mediso AnyScan SPET / CT / PET

GE Discovery NM/CT 670 Pro

Siemens Symbia Intevo

Philips Brightview

CT-AC in SPET

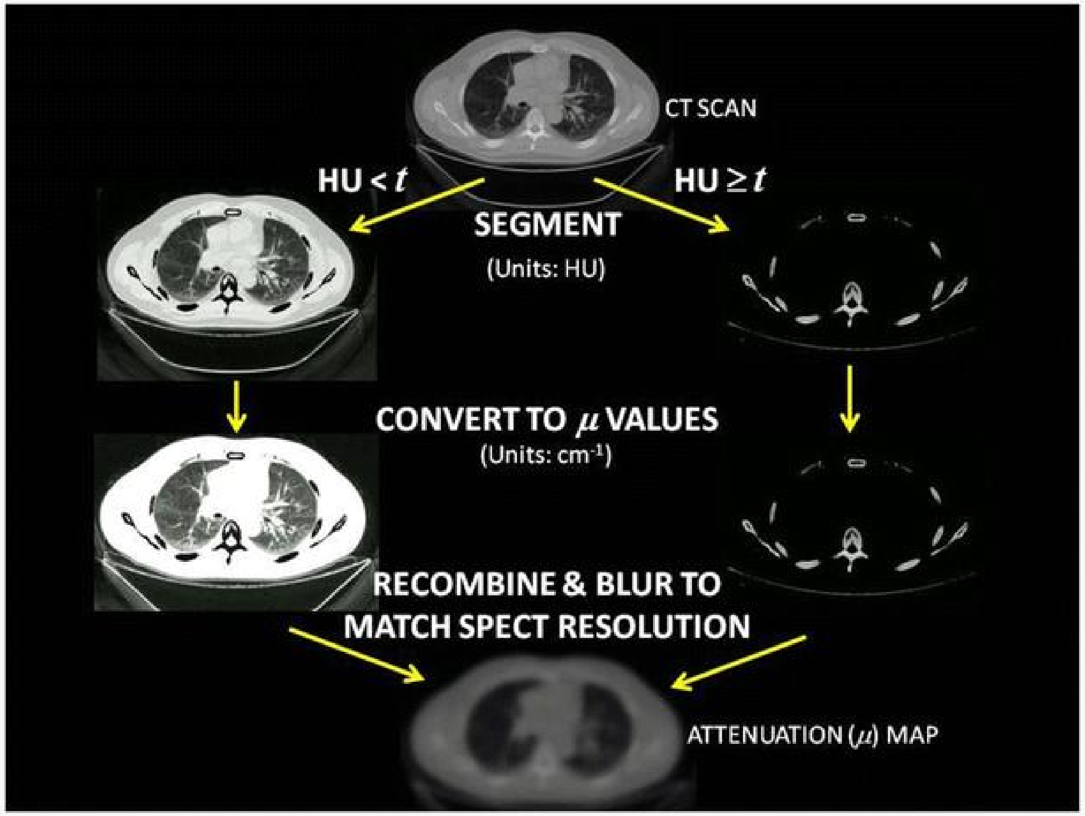

Fig. 5

The steps involved in converting from a CT scan to linear attenuation map are shown. The threshold value *t* is usually chosen in the range 0–100 HU

Eur J Nucl Med Mol Imaging. 2014 May;41 Suppl 1:S17-25. doi: 10.1007/s00259-013-2542-4. Epub 2013 Sep 14.

Quantitative SPECT/CT: SPECT joins PET as a quantitative imaging modality.

Bailey DL[1], Willowson KP.

Quantitative SPET

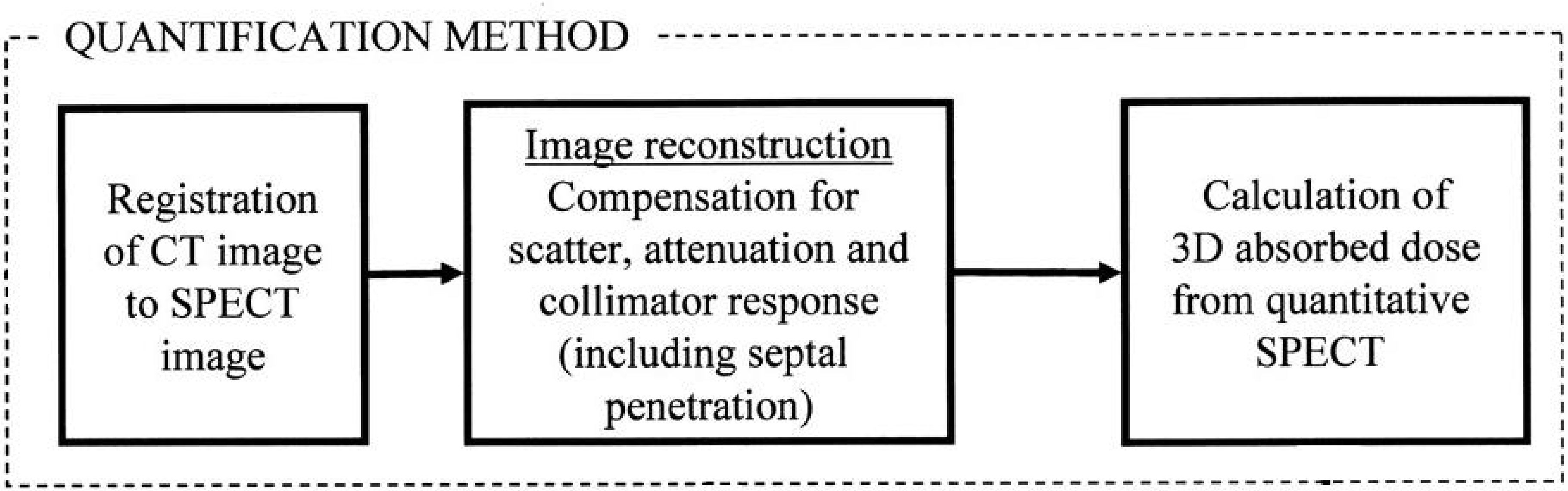

Michael Ljungberg, J Nucl Med 2002; 43:1101–1109

Quantitative SPET - corrections

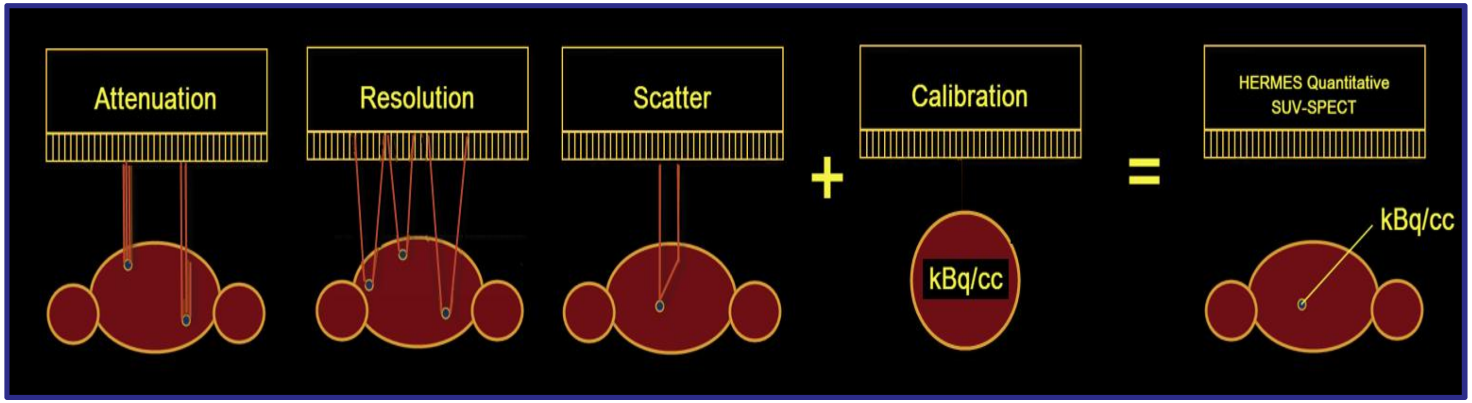

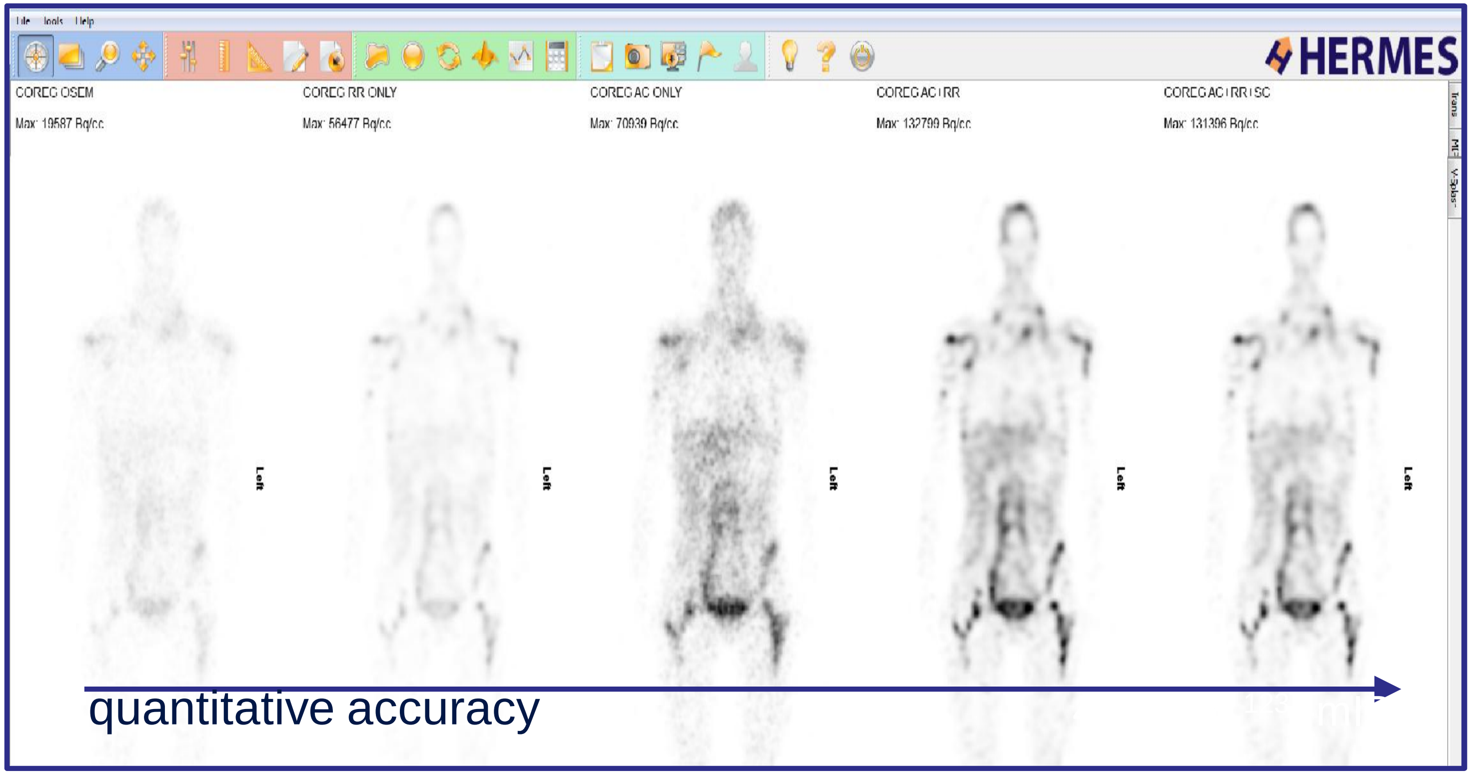

xSPET reconstruction

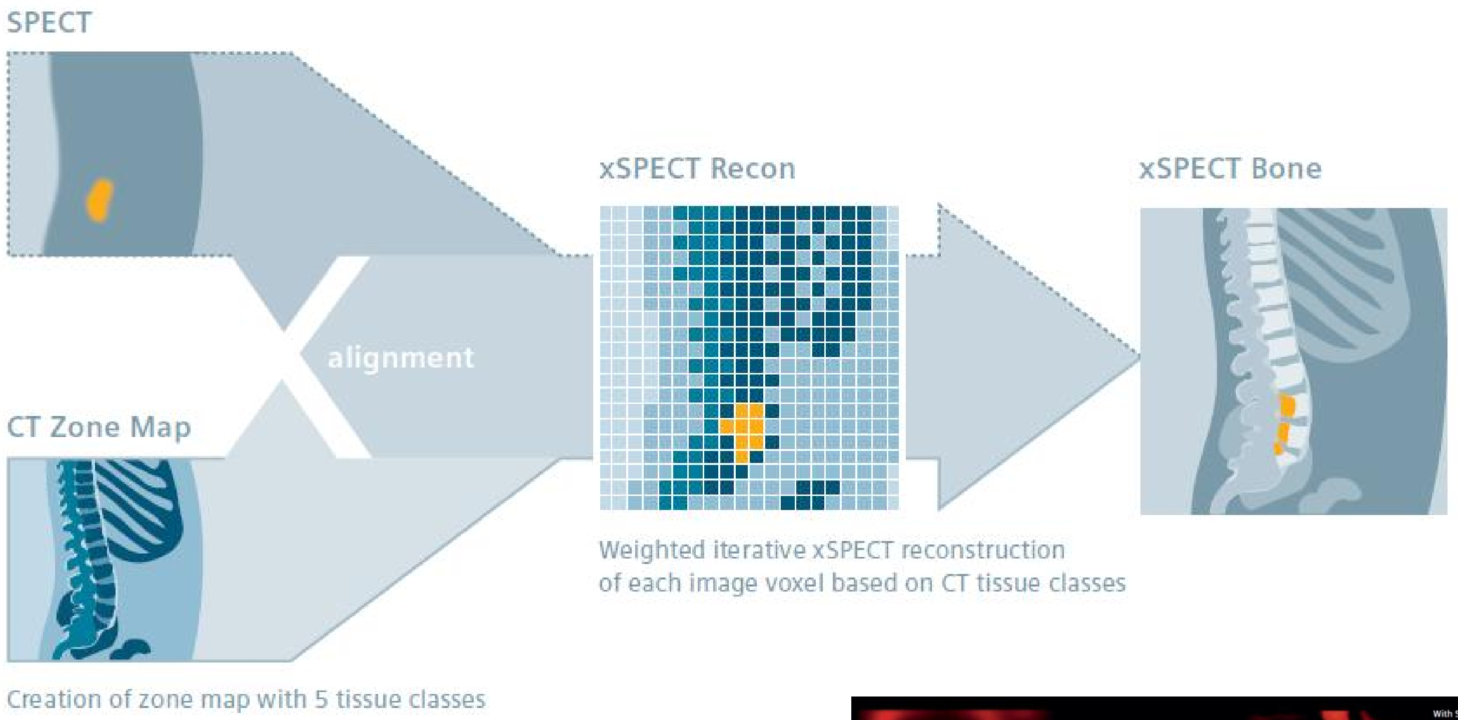

SIEMENS

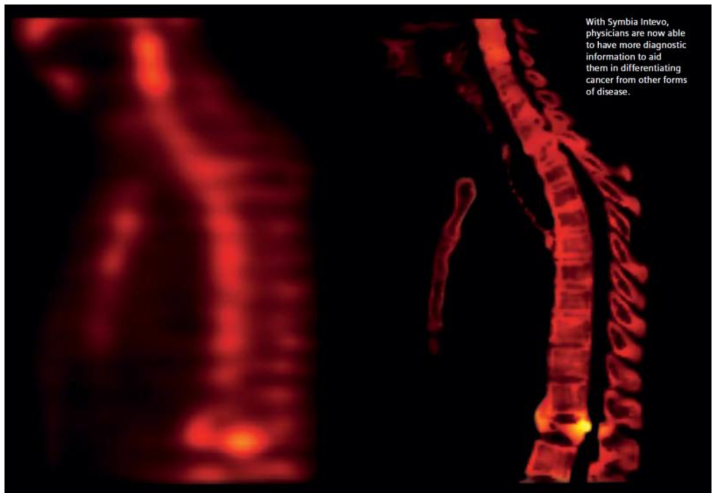

NaI+PMT vs new CZT detector

Anger-camera

CZT-camera

^{99m}Tc (140keV)

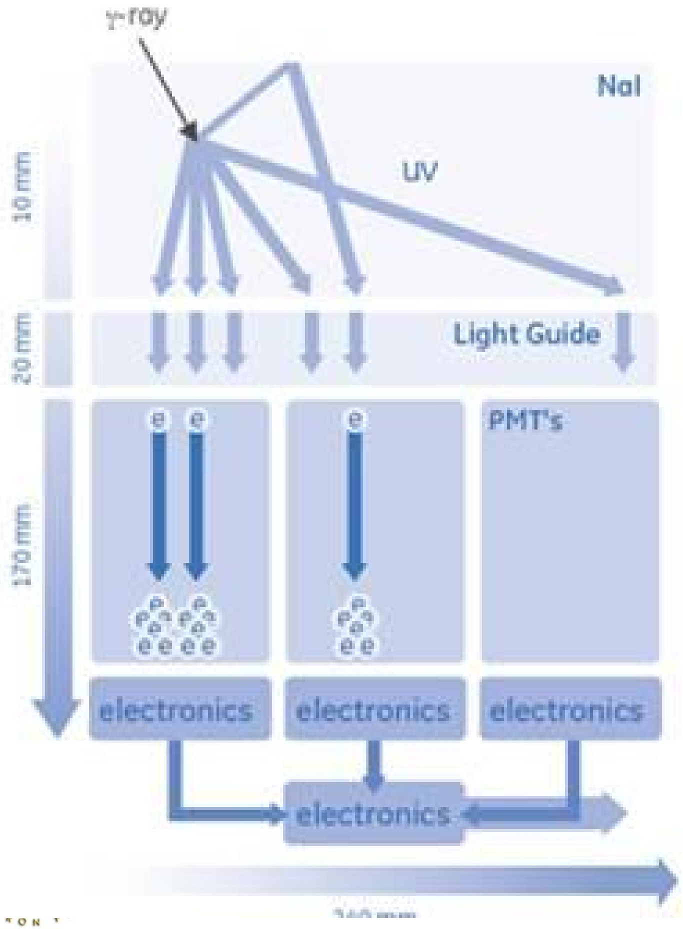

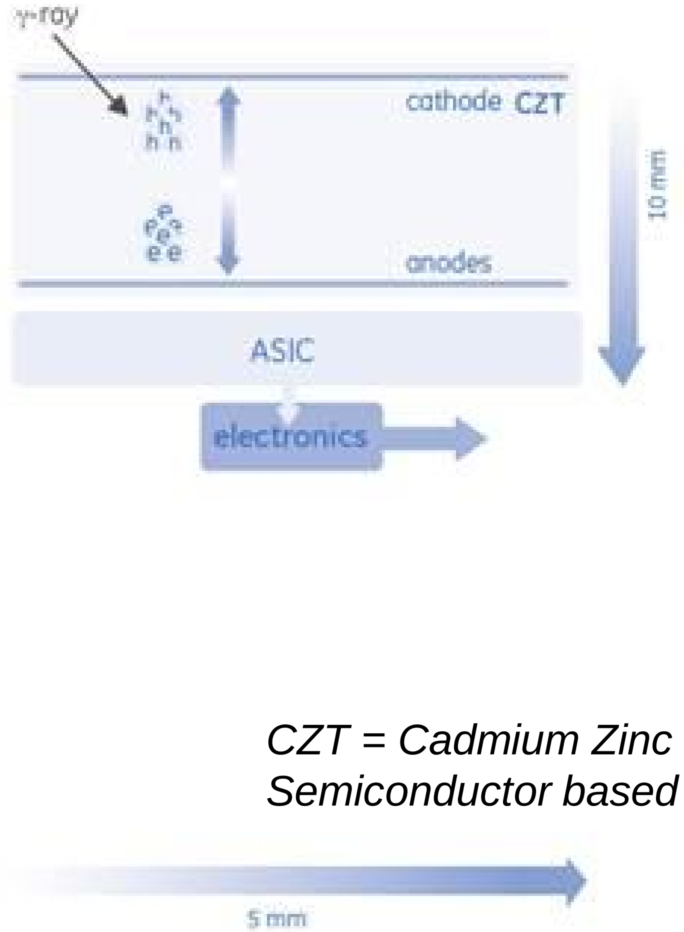

CZT = Cadmium Zinc Telluride
Semiconductor based detector

NaI+PMT vs CZT

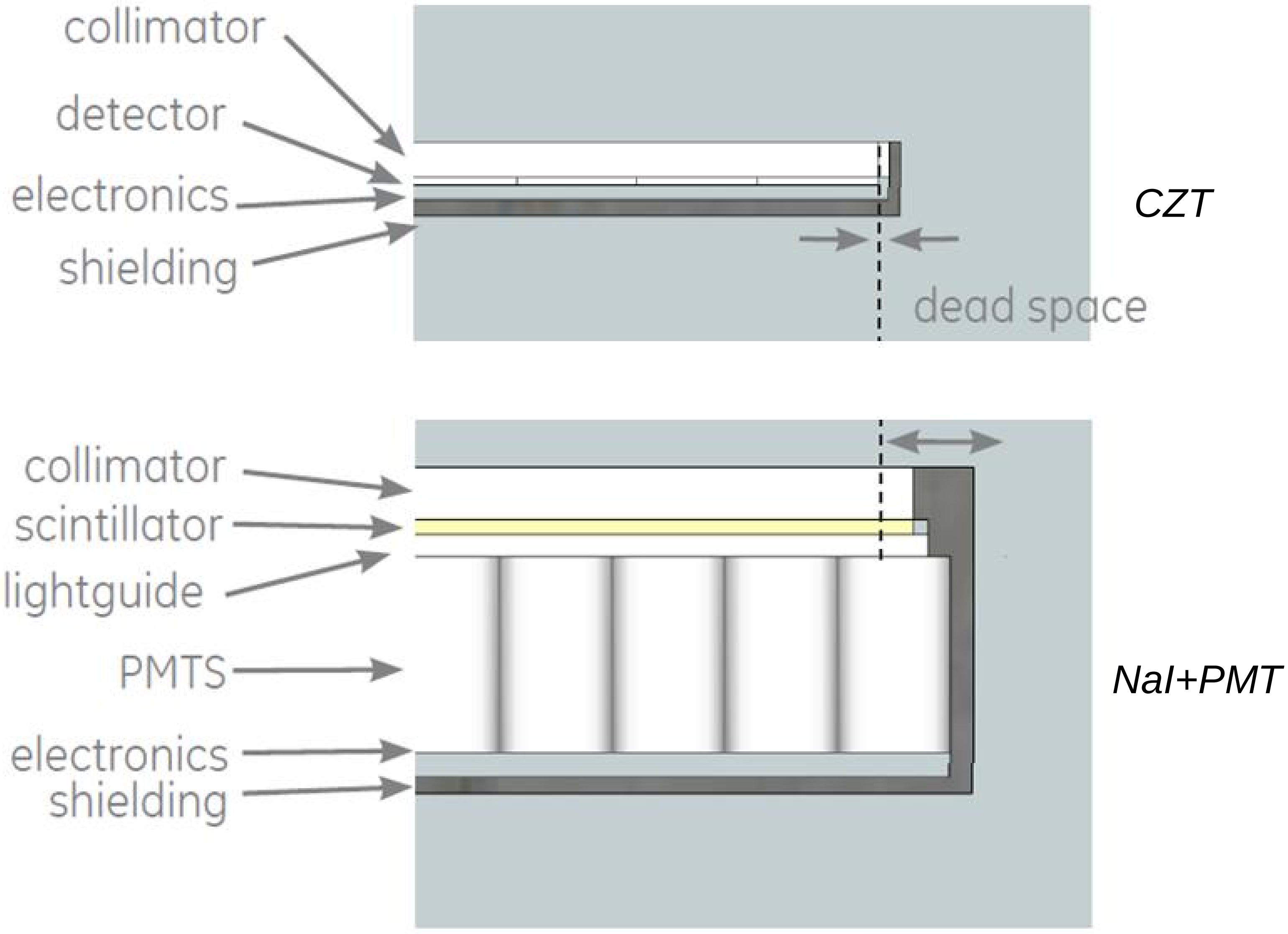

CZT- SPET/CT

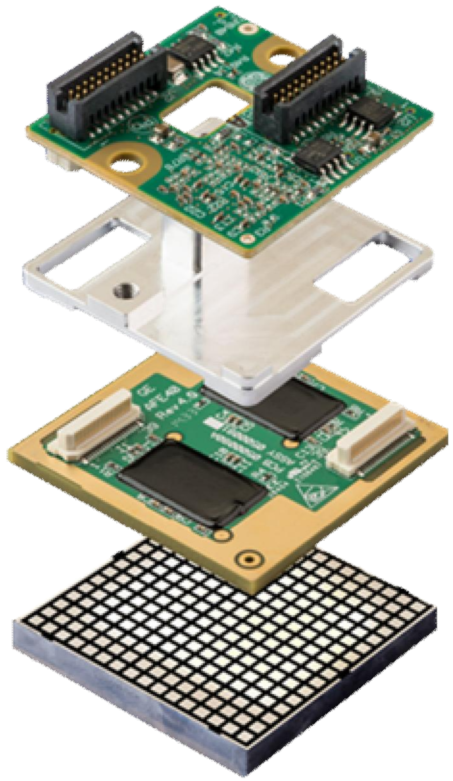

GE Discovery NM/CT 670 CZT
Installed at TUH in late 2017

Energy resolution (NaI vs CZT)

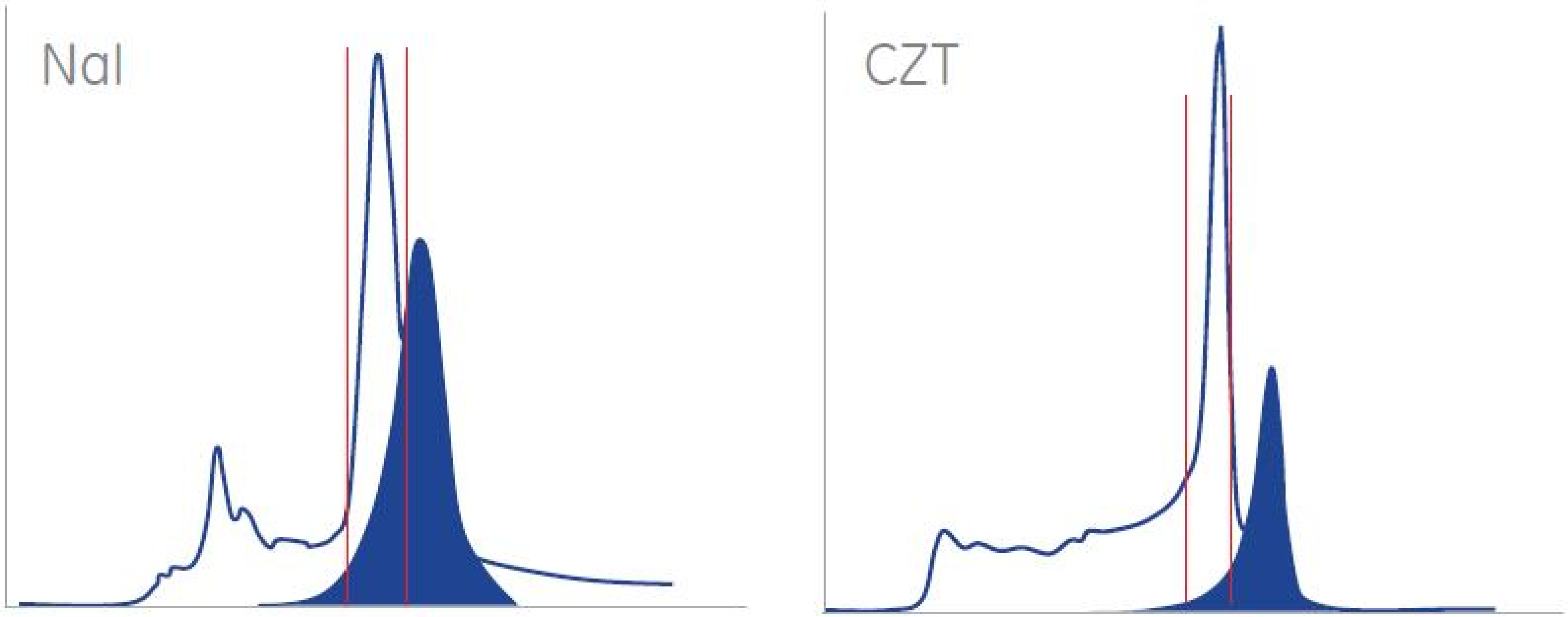

Overlay of ^{99m}Tc and ^{123}I spectra, showing greater crosstalk between the two peaks for the NaI detector with its poorer energy resolution and wider energy window.

CZT FWHM ~ 6 %, theoretical min1.5 %

NaI FWHM ~ 10 %, theoretical min 7 %

Cardiac Procedure

Conventional SPECT/CT

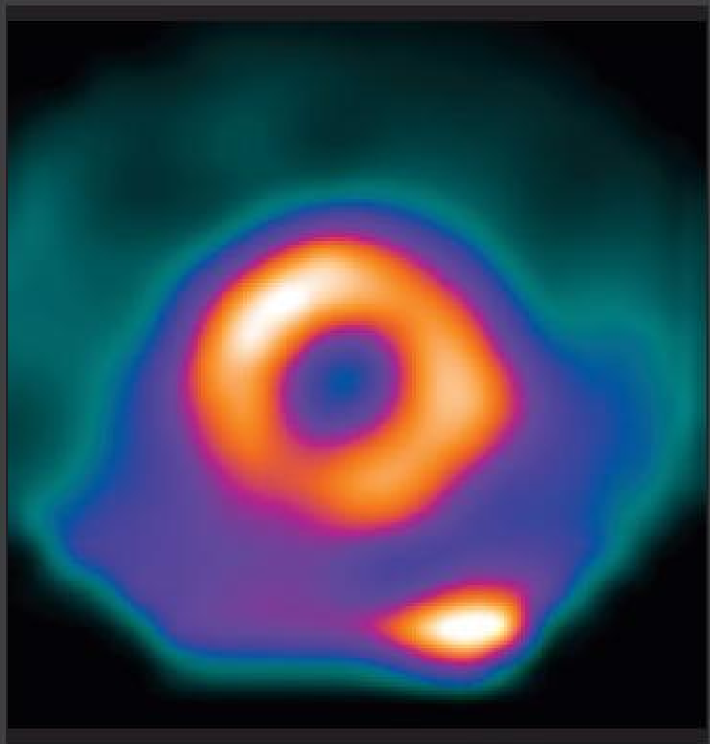

10 min

Discovery NM/CT 670 CZT

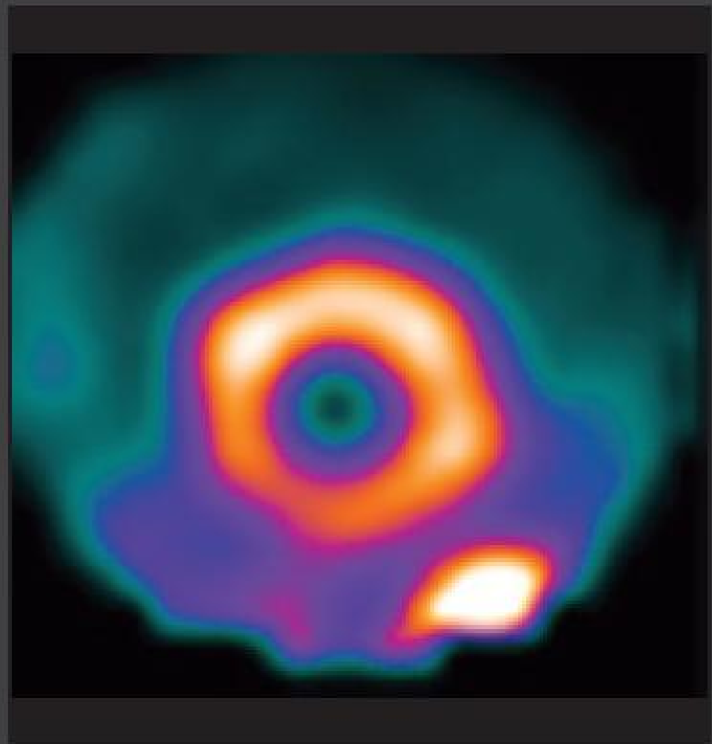

10 min

Positron Emission Tomography

β^+ Emission and Annihilation

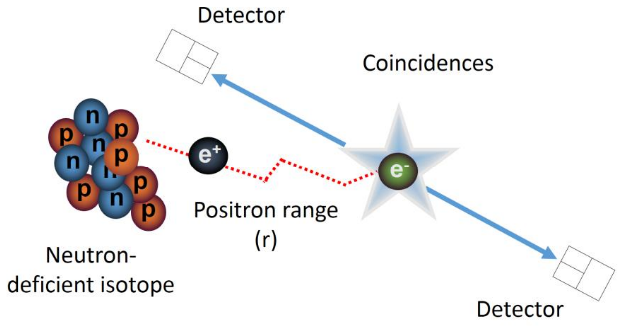

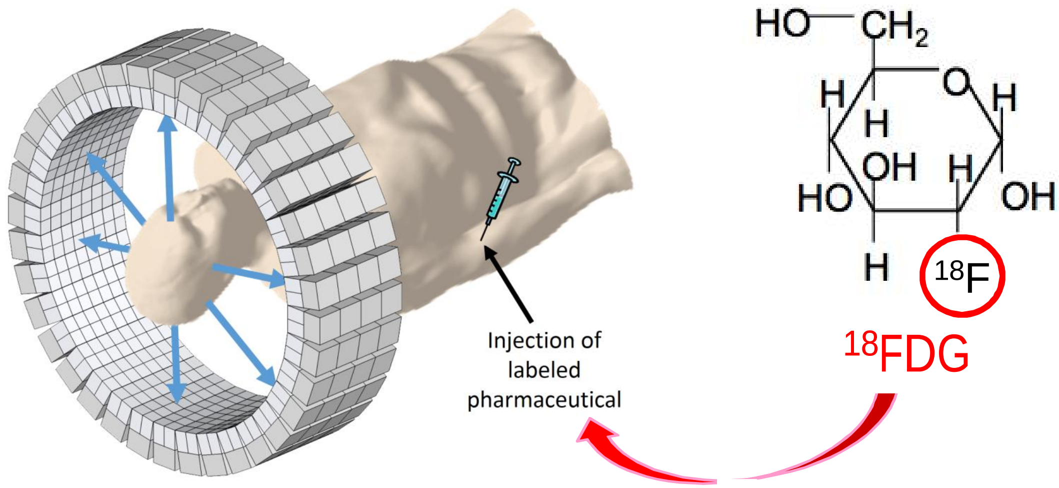

Parallel projections

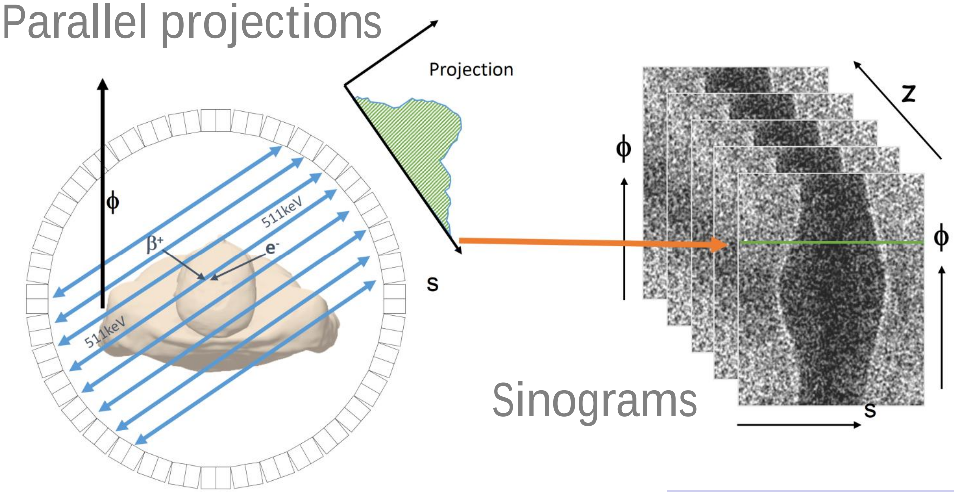

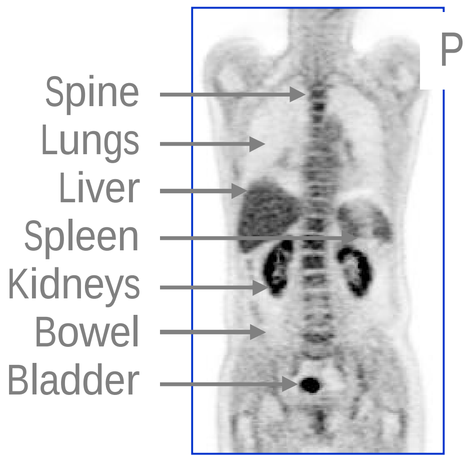

Modeling

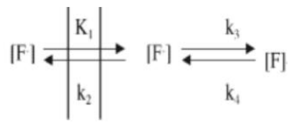

DW Townsend, Singapore

PET - detection

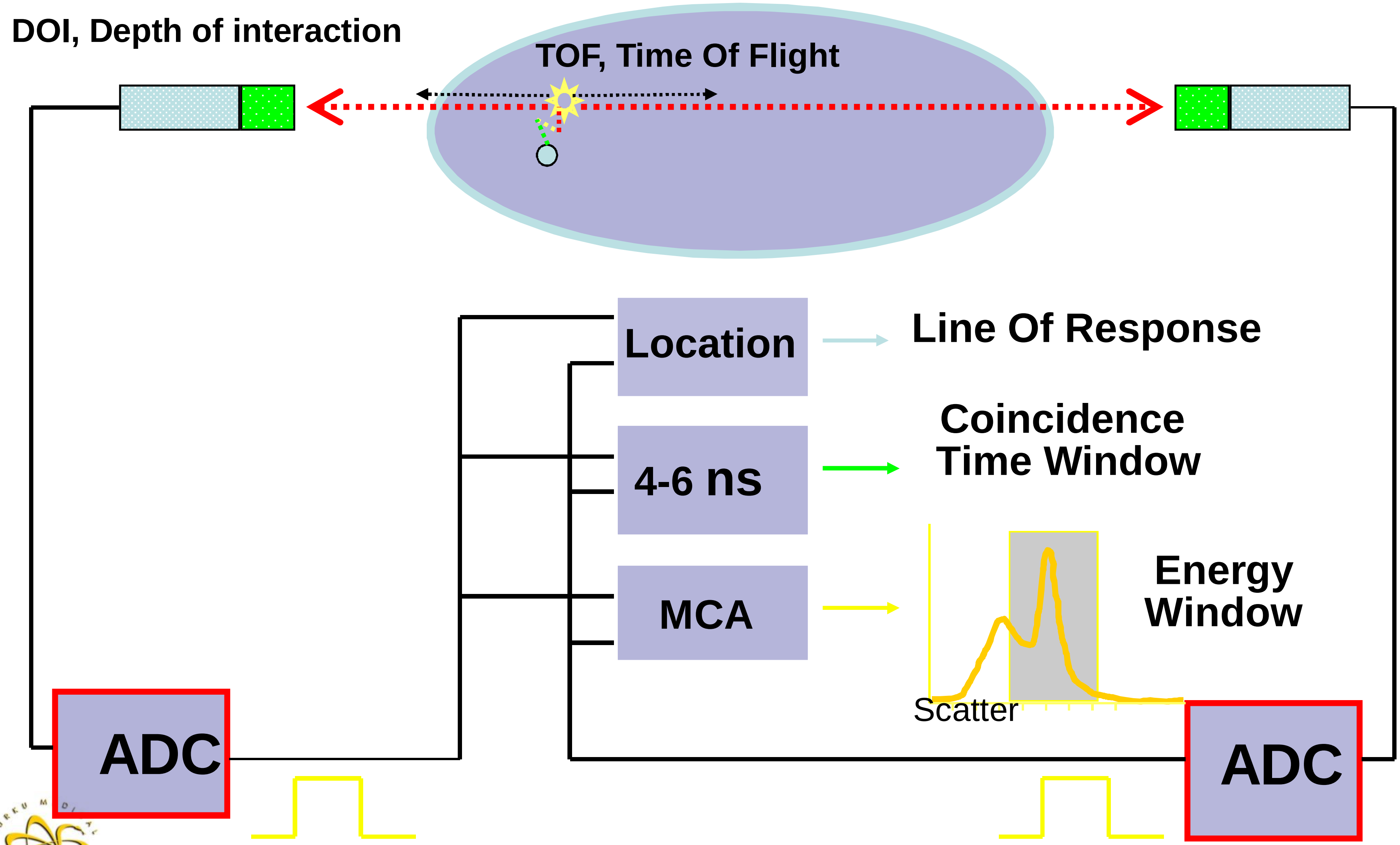

Spatial Resolution

$$FWHM = a\sqrt{(d/2)^2 + b^2 + (0.0022D)^2 + r^2}$$

Reconstruction **Geometric** **Coding** **Non-Collinearity** **Positron Range**

Block Detectors

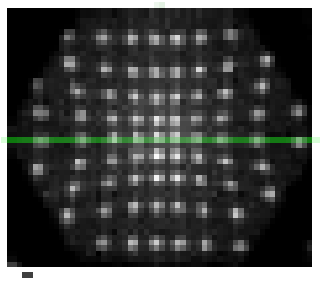

Panel Detectors

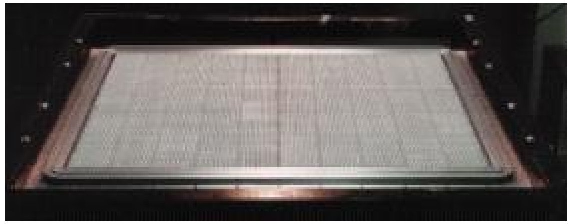

PMTs

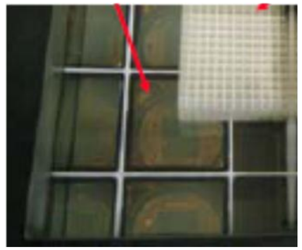

GE : DISCOVERY
BGO

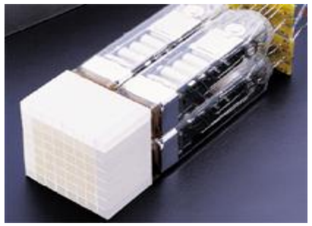

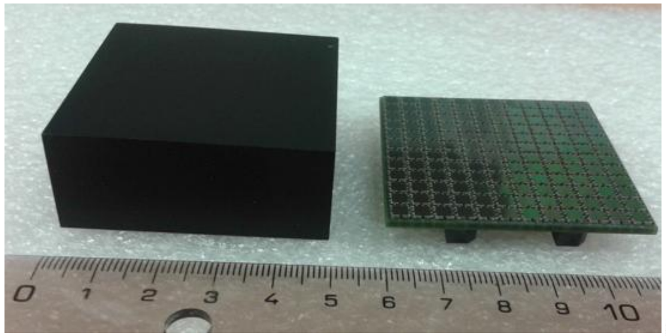

CTI / SIEMENS
LSO

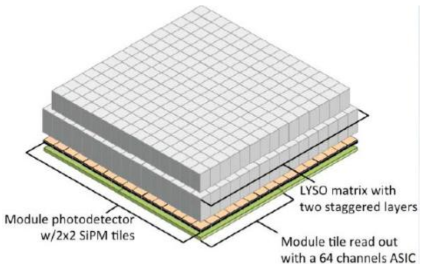

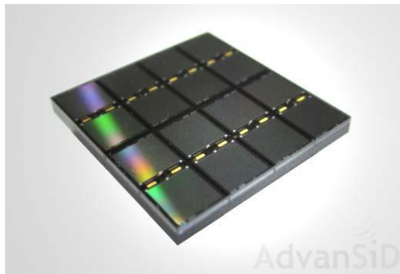

CTI /SIEMENS
BIOGRAPH HiREZ
LSO

Monolite crystal (three 6 mm layers → DOI)
A 12 mm thick black painted trapezoidal (3x6mm) LYSO coupled to 12x12 standard SiPM-SensL array,
MindView brain insert

SiPM

b = 0 individual coupling

Partial Volume (PV) effect

effect of resolution and/or motion

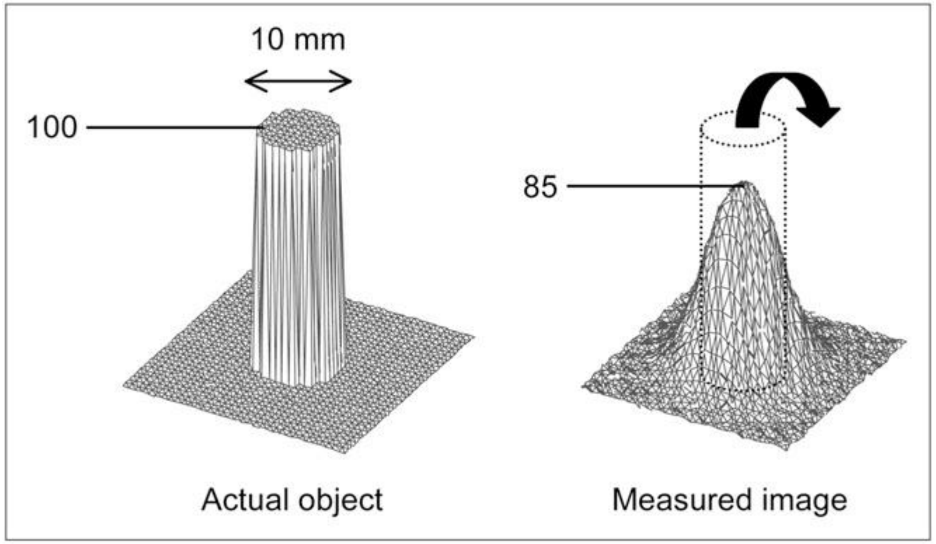

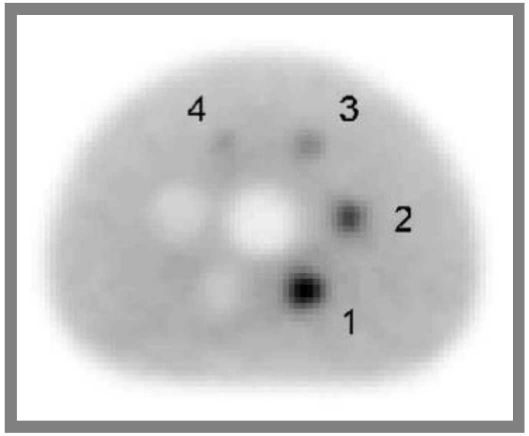

Approaches to PV correction

- iterative deconvolution (subject to noise)
- account for known anatomy (from MRI)
  - introduce an anatomical prior during reconstruction
  - apply correction based on anatomy post-reconstruction

Soret et al. JNM, 48:932-945, 2007
Erlandsson et al. Phys Med Biol 2012; 57: R119

Time Of Flight PET

TOF information can be used in the Reconstruction of the PET data to constraint the possible locations of the annihilation site along the line

Reconstruction without TOF information assumes that all the possible locations of the annihilation site along the line are equally likely.

TOF

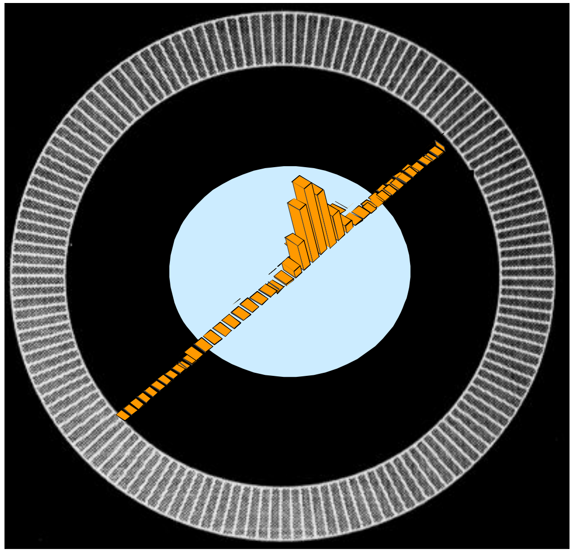

$$\Delta x = \frac{c\,\Delta t}{2}$$

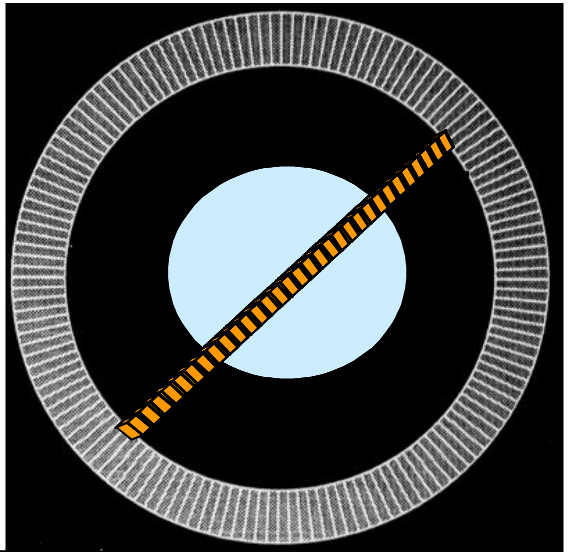

NON TOF

$$\frac{SNR_{TOF}}{SNR} = \sqrt{\frac{2D}{c\,\Delta t}} = \sqrt{\frac{D}{\Delta x}}$$

	Line	SNR GAIN	
Δt psec	Δx mm	D=20 cm	D=35 cm
50	0.75	5.2	6.8
300	4.5	2.1	2.8
500	7.5	1.6	2.2
650	9.75	1.4	1.9

Depth Of Interaction, DOI

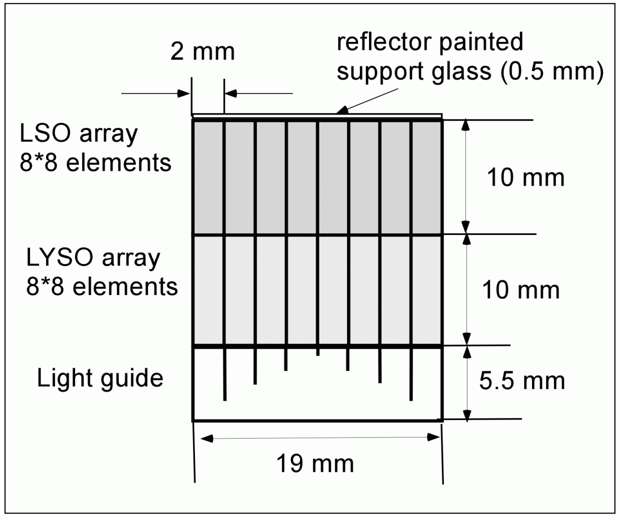

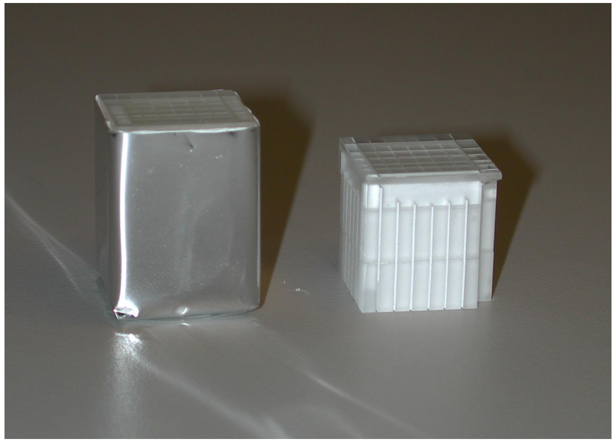

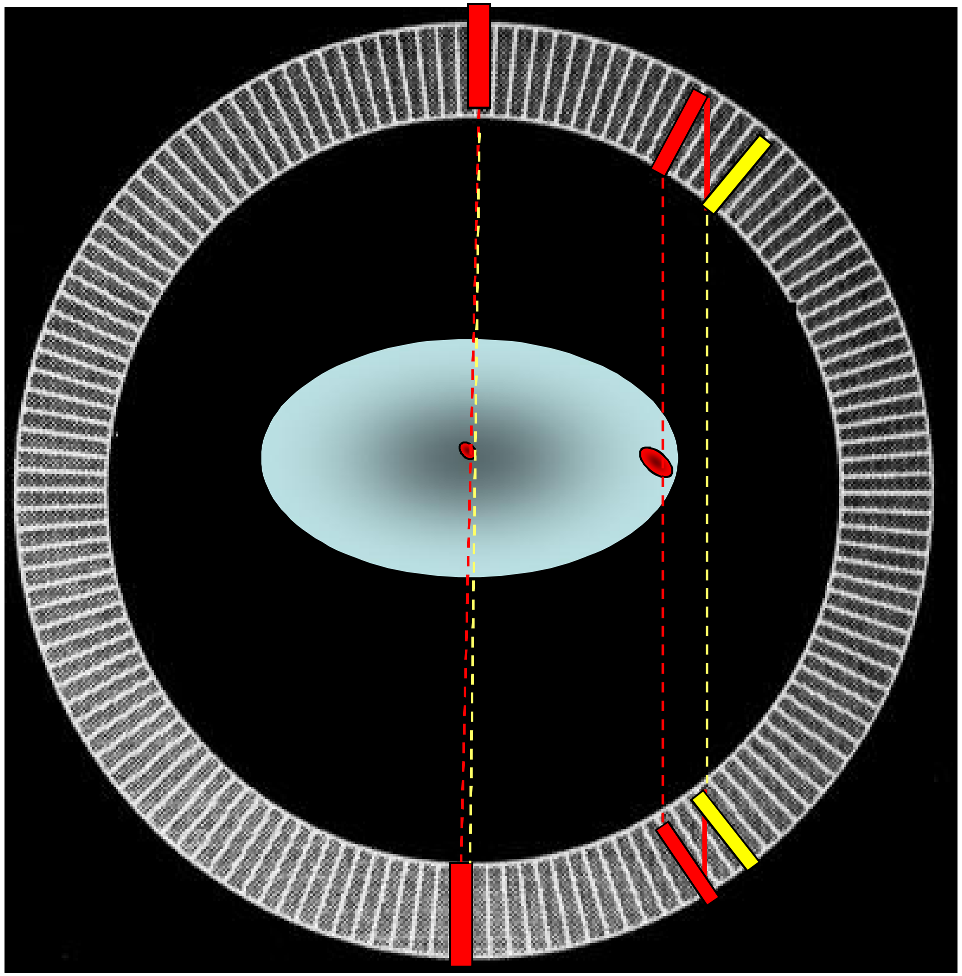

- Bore diameter
- Crystal length

Spatial resolution
degrades towards edges

PET / CT or PET / MR?

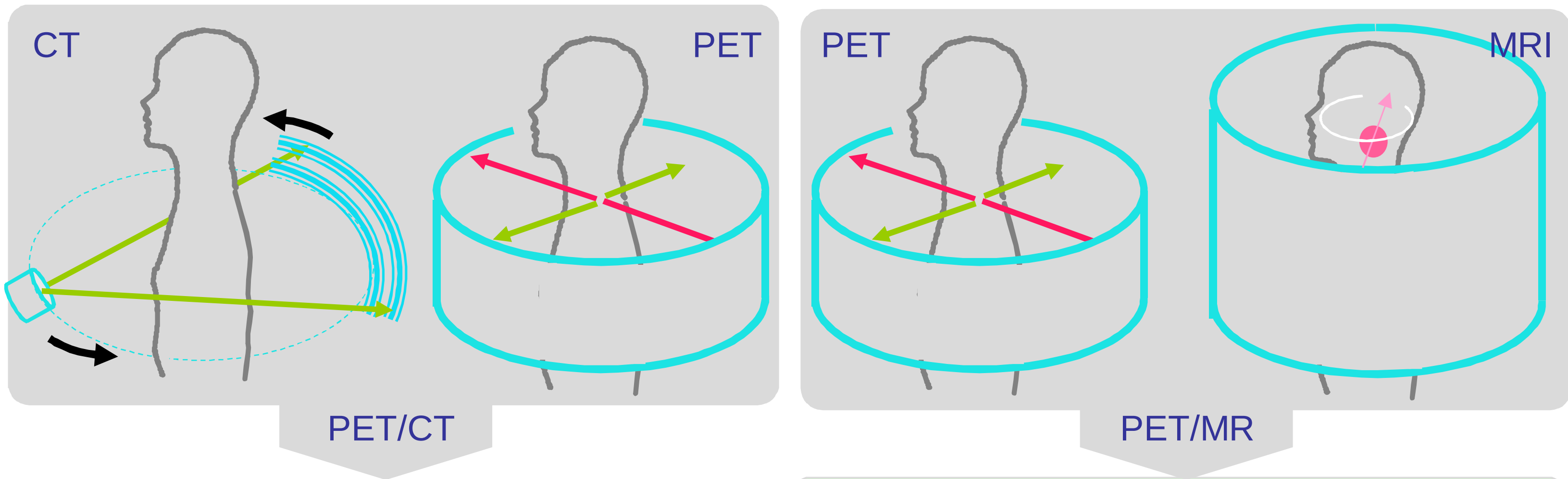

	PET/CT	PET/MR
pro	High-resolution anatomy Best possible, **intrinsic co-registration** Accurate attenuation correction **Fast** whole-body imaging	High **soft tissue contrast** Oblique image planes (“**no-dose tilt**”) **Quasi-simultaneous** imaging Less radiation dose (MR = 0)
con	**Patient exposure from CT** **Motion-induced misalignment** Not simultaneous	**MR-compatible** PET detector MR-based attenuation correction Clinical and research **applications** Limited sensitivity for pulmonary lesions

Modified from T Bayer

Respiratory motion: 4D PET/CT

When scanner resolution and correction algorithms get better
Errors from breathing motion is to be corrected.

Difference in the acquisition time in CT and PET.
CT in breath hold and PET in free breathing

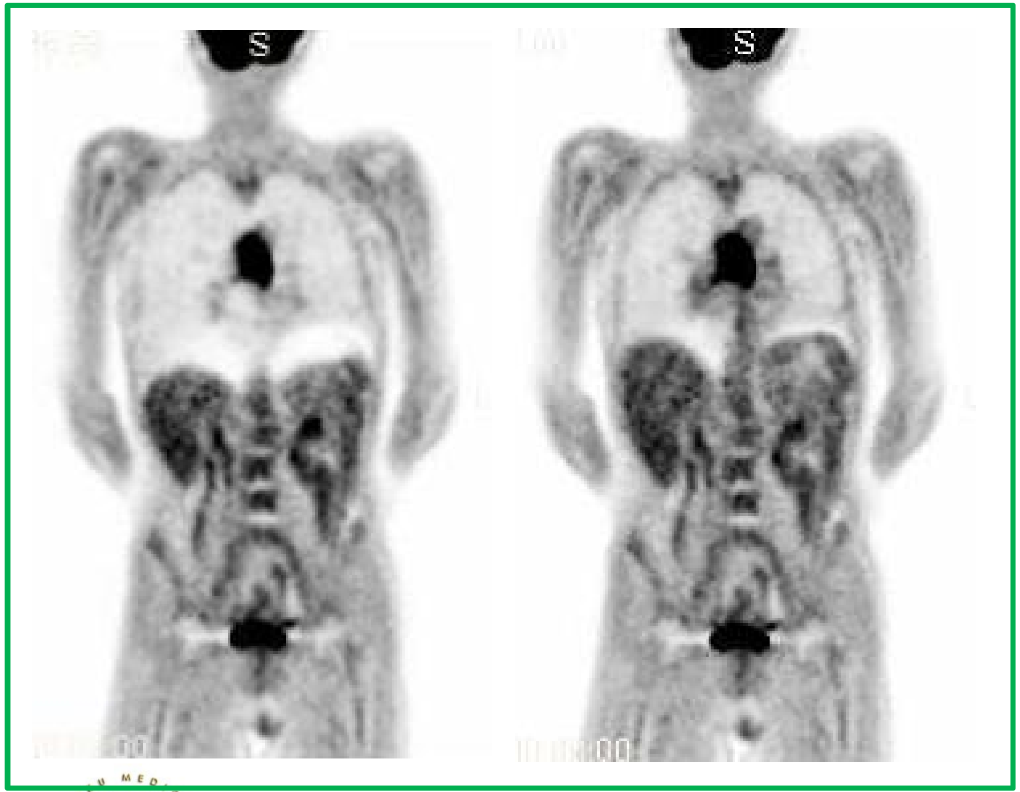

D Visvikis, et al; Eur J Nucl Med 2003, 30(3), 344-353

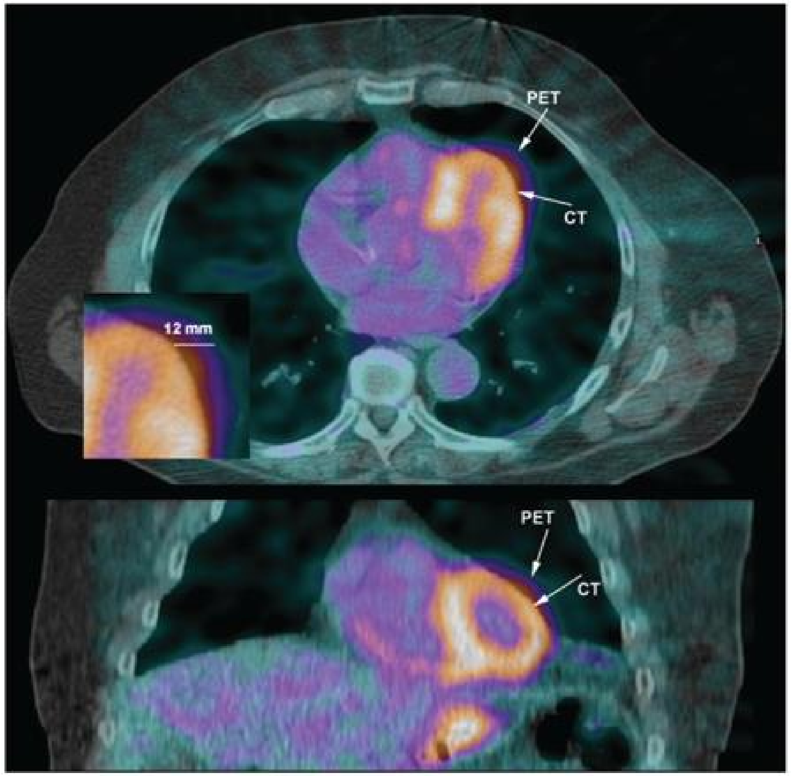

K Lance Gould, et al; J Nucl Med 2007, 48, 1112-1121

RPM Respiratory Gating™ System

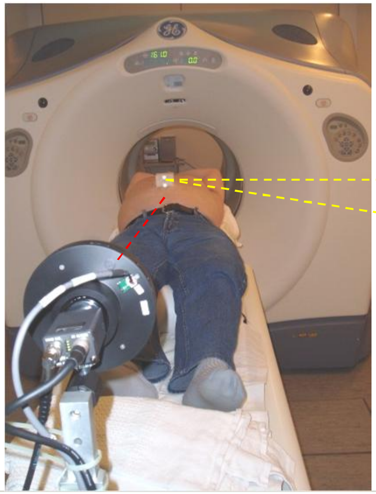

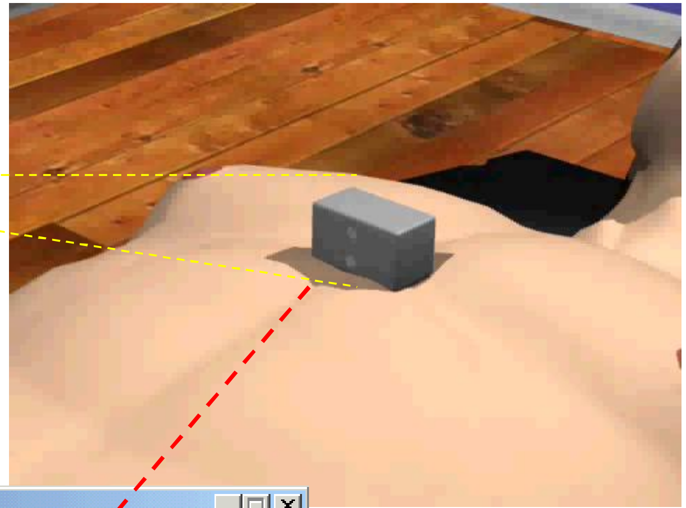

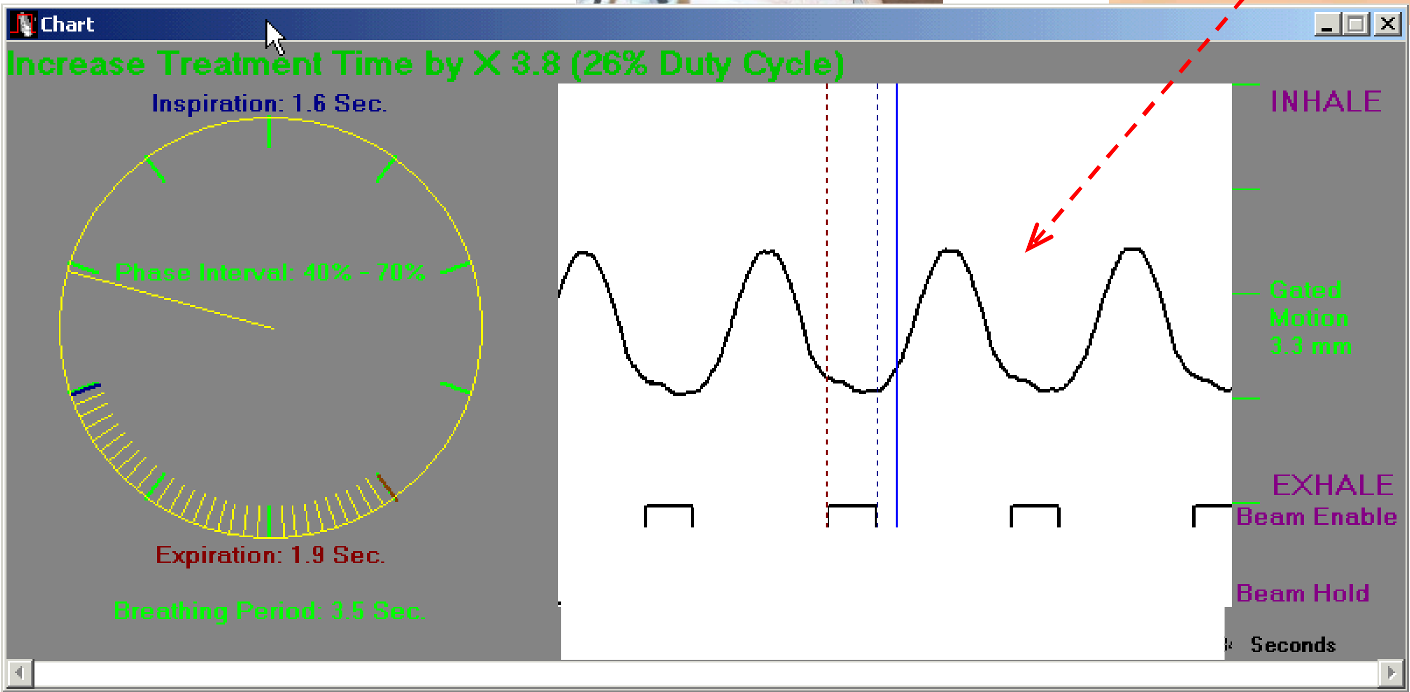

TM : Varian Medical System
Gating School Copenhagen

PET/CT systems with 4D → Lesion Detectability

Conventional PET/CT systems with
Static acquisitions

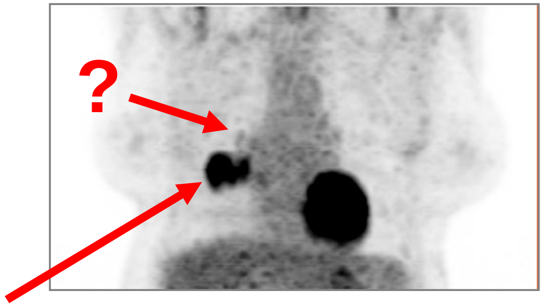

Primary Tumor

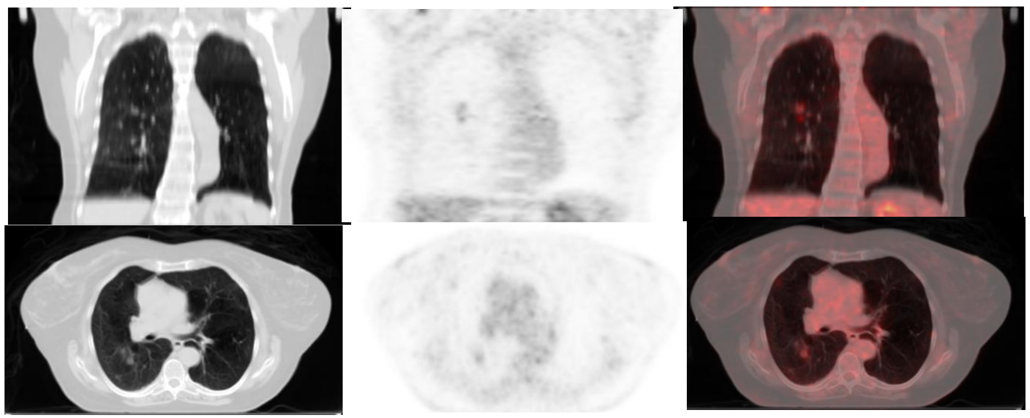

Questionable on CT and appears like normal tissue (same activity) ?

PET/CT Systems with **4D**
Respiratory Gating

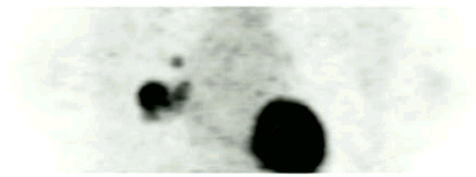

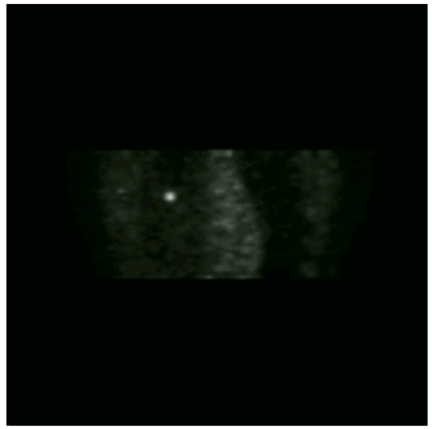

Courtesy of Holyname Hospital

Images courtesy of Holy Name Hospital

MoCo from Static CT and gated PET

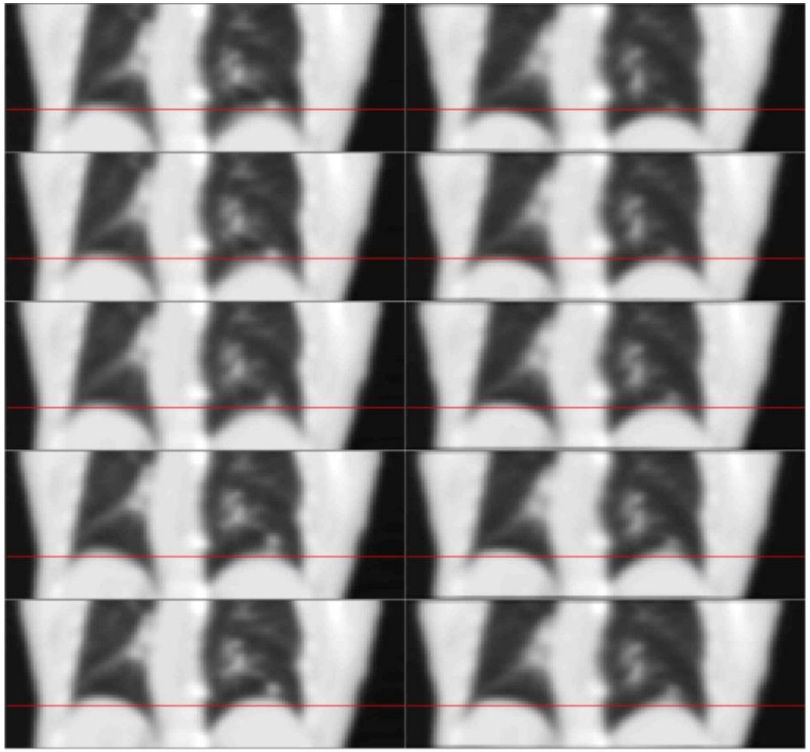

(a) (b)

Gated CT JRM-Wrap CT

Algorithm 1: Joint PET penalized maximum-likelihood motion estimation/image reconstruction

Input: Gated PET data $(\boldsymbol{g}_l)_{l=1}^{n_g}$, attenuation map $\boldsymbol{\mu}$, image and motion smoothing priors β and γ

Output: PET image coefficients $\boldsymbol{f}$, B-spline motion parameter $\boldsymbol{\theta}$

initialization ;
$\boldsymbol{\theta} \leftarrow \boldsymbol{0}$;
$\boldsymbol{f} \leftarrow \text{M-MLEM}(\boldsymbol{g}_1, \boldsymbol{\mu}, \beta)$;
for $r = 1, \ldots, \text{MaxIter}$ **do**
  motion estimation ;
  for $q = 1, \ldots, q_{\max}$ **do**
    for $l = 1, \ldots, n_g$ **do**
      for $C \in \{X, Y, Z\}$, $\boldsymbol{h} \in \{\boldsymbol{f}, \boldsymbol{\mu}\}$ **do**
        $\boldsymbol{J}_{\boldsymbol{h}}^C \leftarrow \text{diag}\left\{\boldsymbol{W}_{\boldsymbol{\alpha}_l}^{\partial C} \boldsymbol{h}\right\} \boldsymbol{\mathcal{B}}$;
      end
      $\boldsymbol{J}_{\boldsymbol{f}} \leftarrow [\boldsymbol{J}_{\boldsymbol{f}}^X, \boldsymbol{J}_{\boldsymbol{f}}^Y, \boldsymbol{J}_{\boldsymbol{f}}^Z]$;
      $\boldsymbol{J}_{\boldsymbol{\mu}} \leftarrow [\boldsymbol{J}_{\boldsymbol{\mu}}^X, \boldsymbol{J}_{\boldsymbol{\mu}}^Y, \boldsymbol{J}_{\boldsymbol{\mu}}^Z]$;
      $\nabla \Lambda_l \leftarrow \boldsymbol{g}_l / \overline{\boldsymbol{g}}_l(\boldsymbol{f}, \boldsymbol{\alpha}_l, \boldsymbol{\mu}) - \boldsymbol{1}$;
      $\nabla_{\boldsymbol{\alpha}_l} L \leftarrow -\tau_l \boldsymbol{J}_{\boldsymbol{\mu}}^\top \boldsymbol{L}^\top \text{diag}\{\boldsymbol{H}_\text{a}^\text{m}(\boldsymbol{\alpha}_l, \boldsymbol{\mu}) \boldsymbol{f}\} \nabla \Lambda_l +$
      $\tau_l \boldsymbol{J}_{\boldsymbol{f}}^\top \boldsymbol{H}_\text{a}(\boldsymbol{W}_{\boldsymbol{\alpha}_l} \boldsymbol{\mu})^\top \nabla \Lambda_l$;
    end
    $\nabla \Phi \leftarrow [\nabla_{\boldsymbol{\alpha}_1} L^\top, \ldots, \nabla_{\boldsymbol{\alpha}_{n_g}} L^\top]^\top + \gamma \nabla V(\boldsymbol{\theta})$;
    $\boldsymbol{t} \leftarrow \text{LBFGS}(\nabla \Phi, \boldsymbol{\theta})$;
    $\delta^\star \leftarrow \arg\max_{\delta \geq 0} \Phi(\boldsymbol{\theta} + \delta \boldsymbol{t})$;
    $\boldsymbol{\theta} \leftarrow \boldsymbol{\theta} + \delta^\star \boldsymbol{t}$;
  end
  image reconstruction ;
  if $\text{mod}(r, r_\text{reinit}) = 0$ **then**
    $\boldsymbol{f} \leftarrow \boldsymbol{1}$;
  end
  $\boldsymbol{\pi} \leftarrow \sum_{l=1}^{n_g} \boldsymbol{H}_\text{a}^\text{m}(\boldsymbol{\alpha}_l, \boldsymbol{\mu})^\top \boldsymbol{1}$;
  for $p = 1, \ldots, p_{\max}$ **do**
    $\boldsymbol{F}^\text{em} \leftarrow \frac{\boldsymbol{f}}{\boldsymbol{\pi}} \sum_{l=1}^{n_g} \boldsymbol{H}_\text{a}^\text{m}(\boldsymbol{\alpha}_l, \boldsymbol{\mu})^\top \frac{\boldsymbol{g}_l}{\overline{\boldsymbol{g}}_l(\boldsymbol{f}, \boldsymbol{\alpha}_l, \boldsymbol{\mu})}$;
    if $\beta > 0$ **then**
      $\boldsymbol{F}^\text{reg} \leftarrow \boldsymbol{F}^\text{reg}(\boldsymbol{f})$;
      $\boldsymbol{f} \leftarrow \arg\max_{\boldsymbol{f} \geq 0} Q^L(\boldsymbol{f}; \boldsymbol{F}^\text{em}) + Q^U(\boldsymbol{f}; \boldsymbol{F}^\text{reg})$;
    else
      $\boldsymbol{f} \leftarrow \boldsymbol{F}^\text{em}$;
    end
  end
end

Maximum-Likelihood Joint Image Reconstruction/Motion Estimation in Attenuation-Corrected Respiratory Gated PET/CT Using a Single Attenuation Map

Alexandre Bousse, Ottavia Bertolli, David Atkinson, Simon Arridge, Sébastien Ourselin, Brian F. Hutton, *Senior Member, IEEE*, and Kris Thielemans, *Senior Member, IEEE*m

IEEE TRANSACTIONS ON MEDICAL IMAGING, VOL. 35, NO. 1, JANUARY 2016

MR Image-based PET MoCo in PET/MR

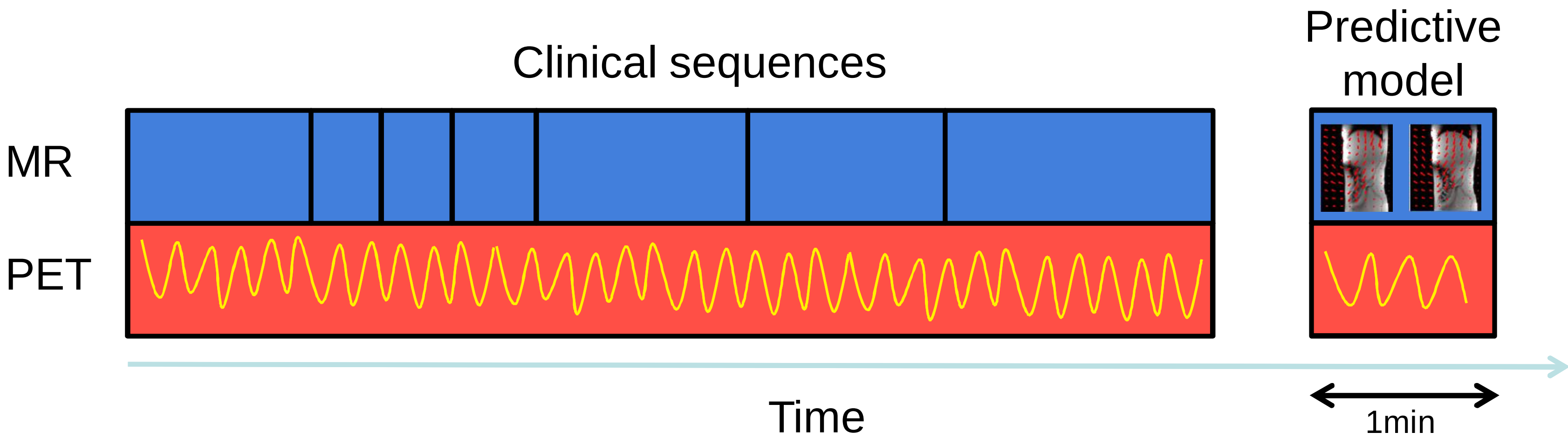

Method:
- Respiratory signal from PET data (PCA)
- Dynamic MR + registration cf PCA signal
  => Motion model for gated PET
- Incorporate motion into PET reconstruction
  => Motion-corrected PET image

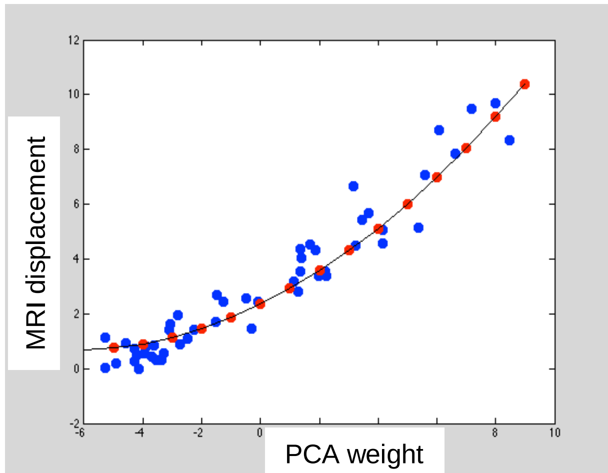

Manber et al. J Nucl Med 2015; 56: 890.
Manber et al. Phys Med Biol 2016; 61: 6515

Example of MoCo

- improved lesion detection and localisation
- artefact reduction
- improved quantification

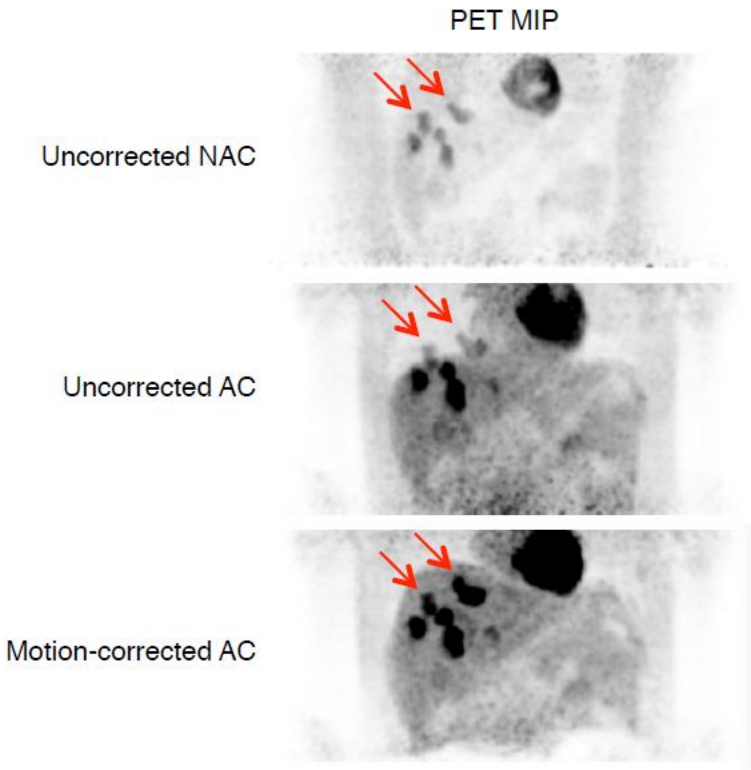

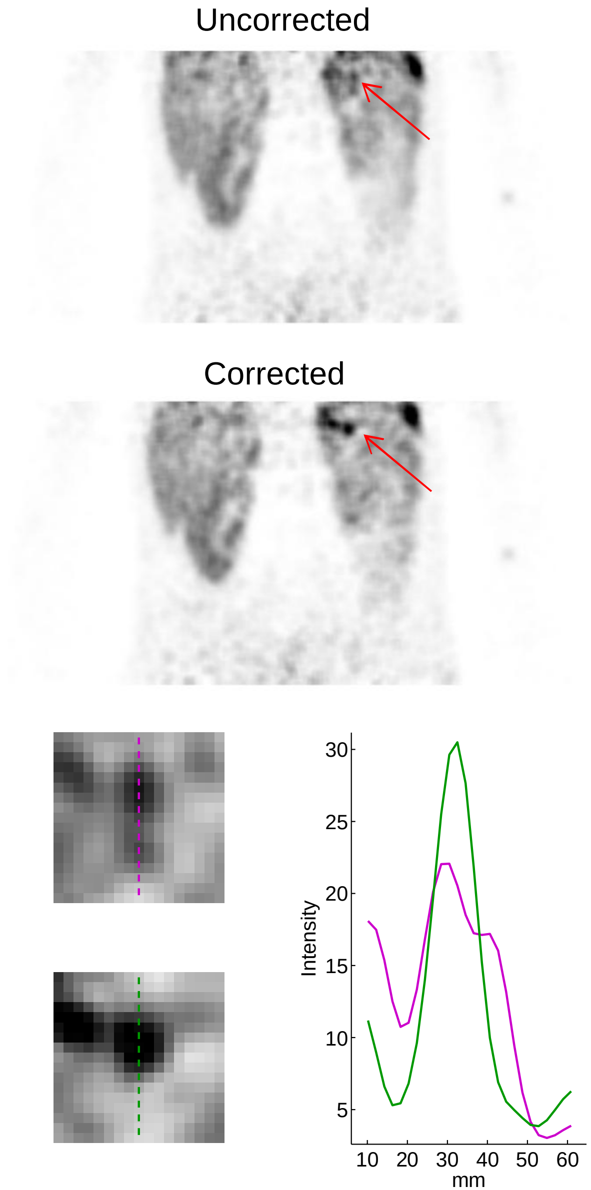

Manber et al. J Nucl Med 2015; 56: 890.
Manber et al. Phys Med Biol 2016; 61: 6515

CT vs MR in Image Segmentation

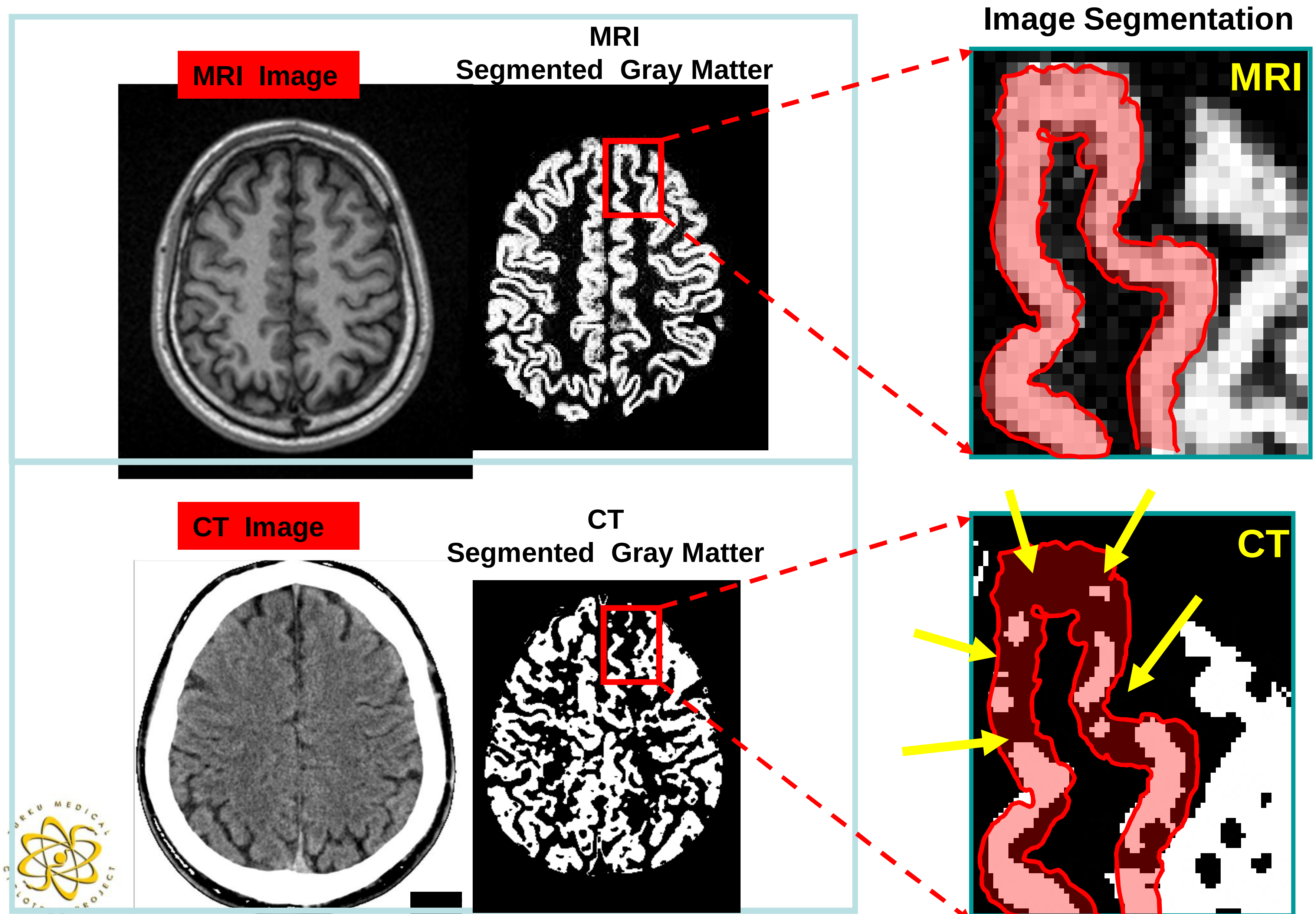

PMT is sensitive to magnetic fields

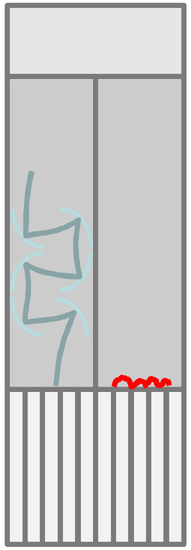

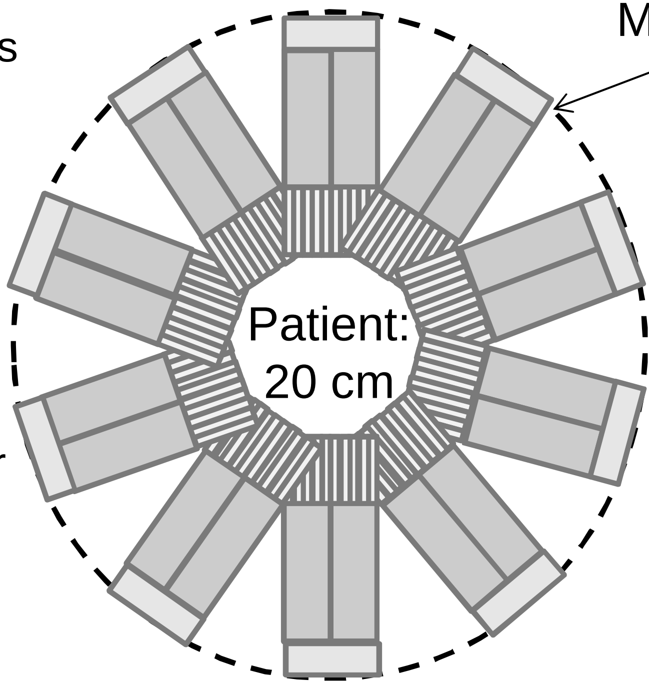

- A conventional PET detector leaves insufficient space for the patient

Replace PMT with SiPM based detector

25 mm crystals

Optical fiber output

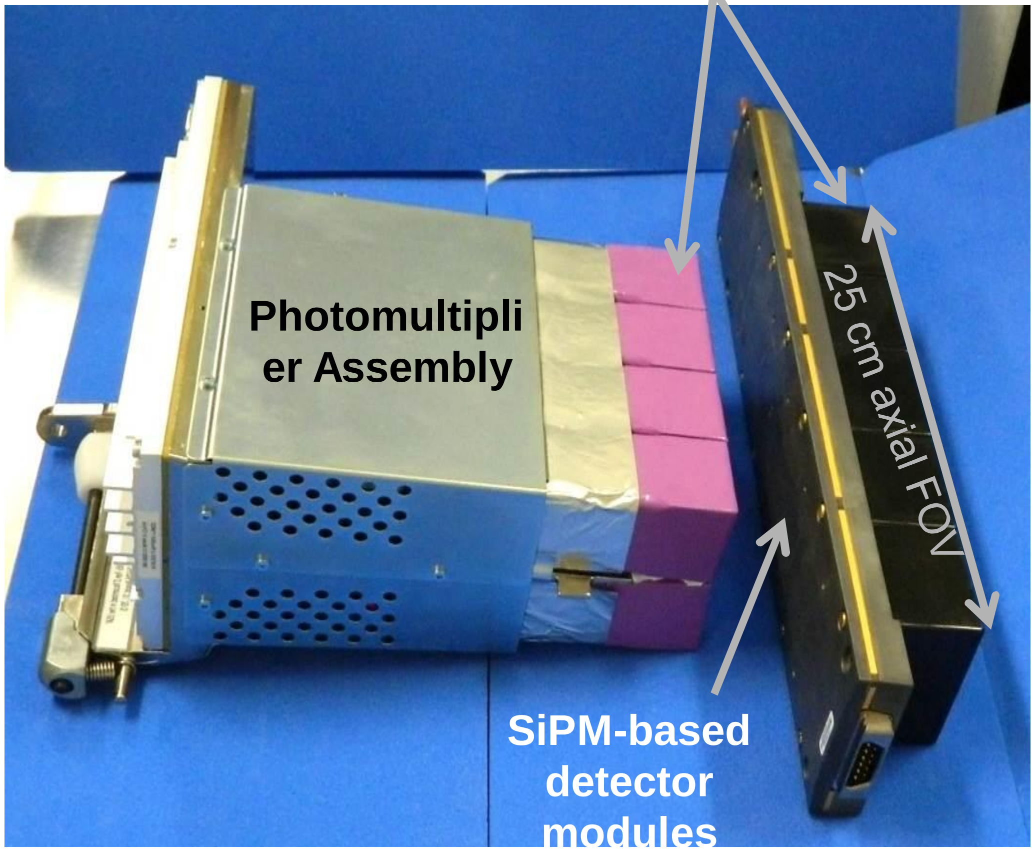

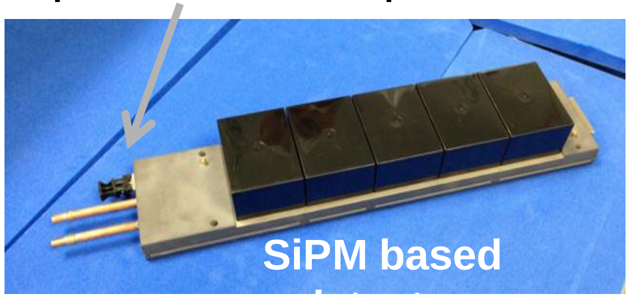

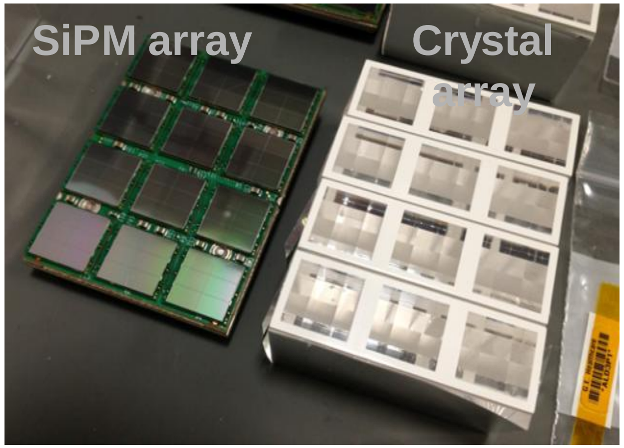

PET/MR: Challenges and Solutions

PET/MR system design (fromThomas Beyer)

MEDICAL UNIVERSITY OF VIENNA

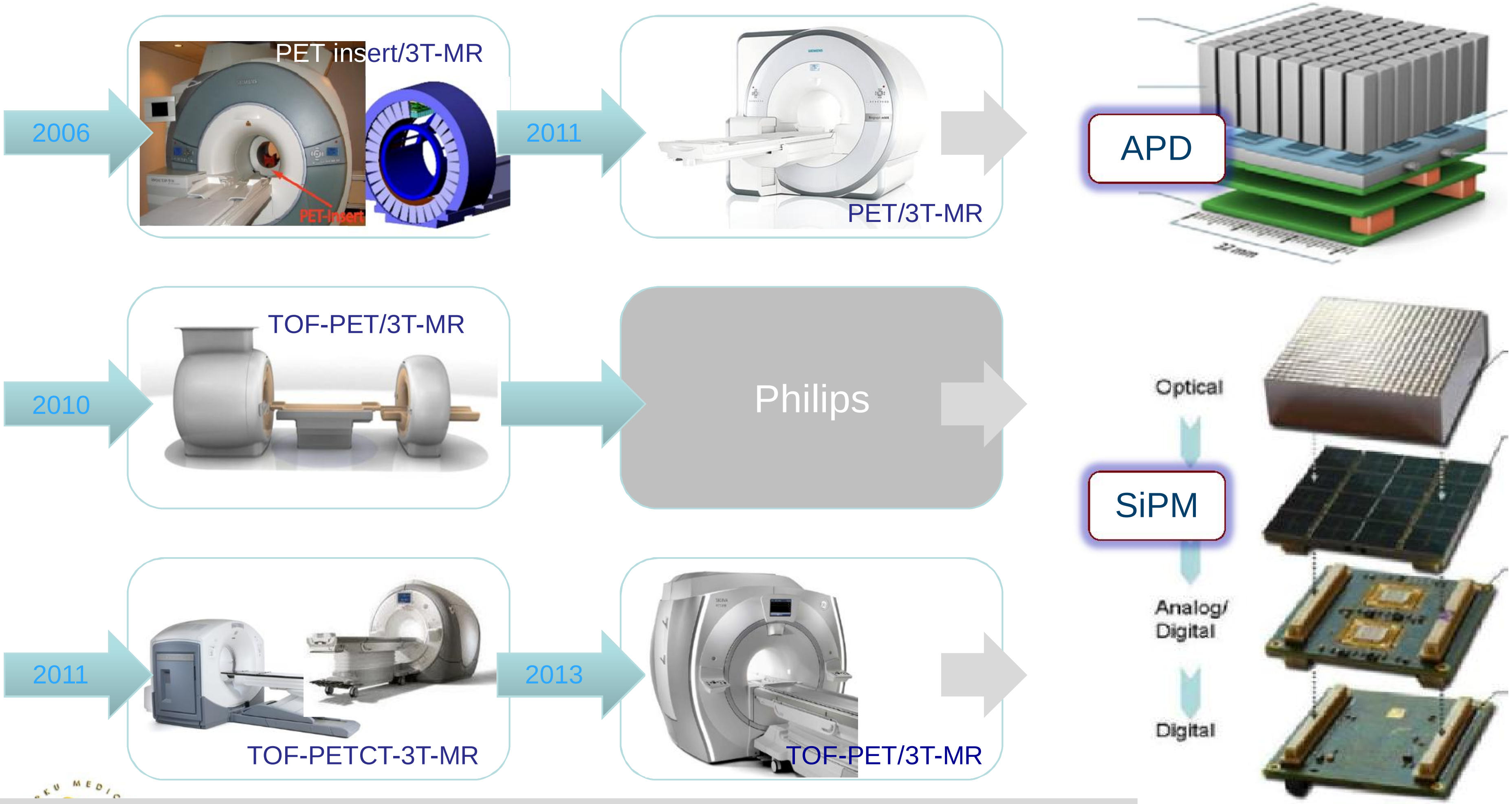

System integration driven by progressive technology.

FUTURE of MMMI

PET 20.0: a cost-efficient, 2mm spatial resolution Total Body PET with point sensitivity up to 22% and adaptive axial FOV of maximum 2.00m

S. Vandenberghe, *E. Mikhalyova, B. Brans, M. Defrise, T. Lahoutte, K. Muylle, R. Van Hole, D. R. Schaart, J. S. Karp; Gent, UC Davies, Delft, U PENN*

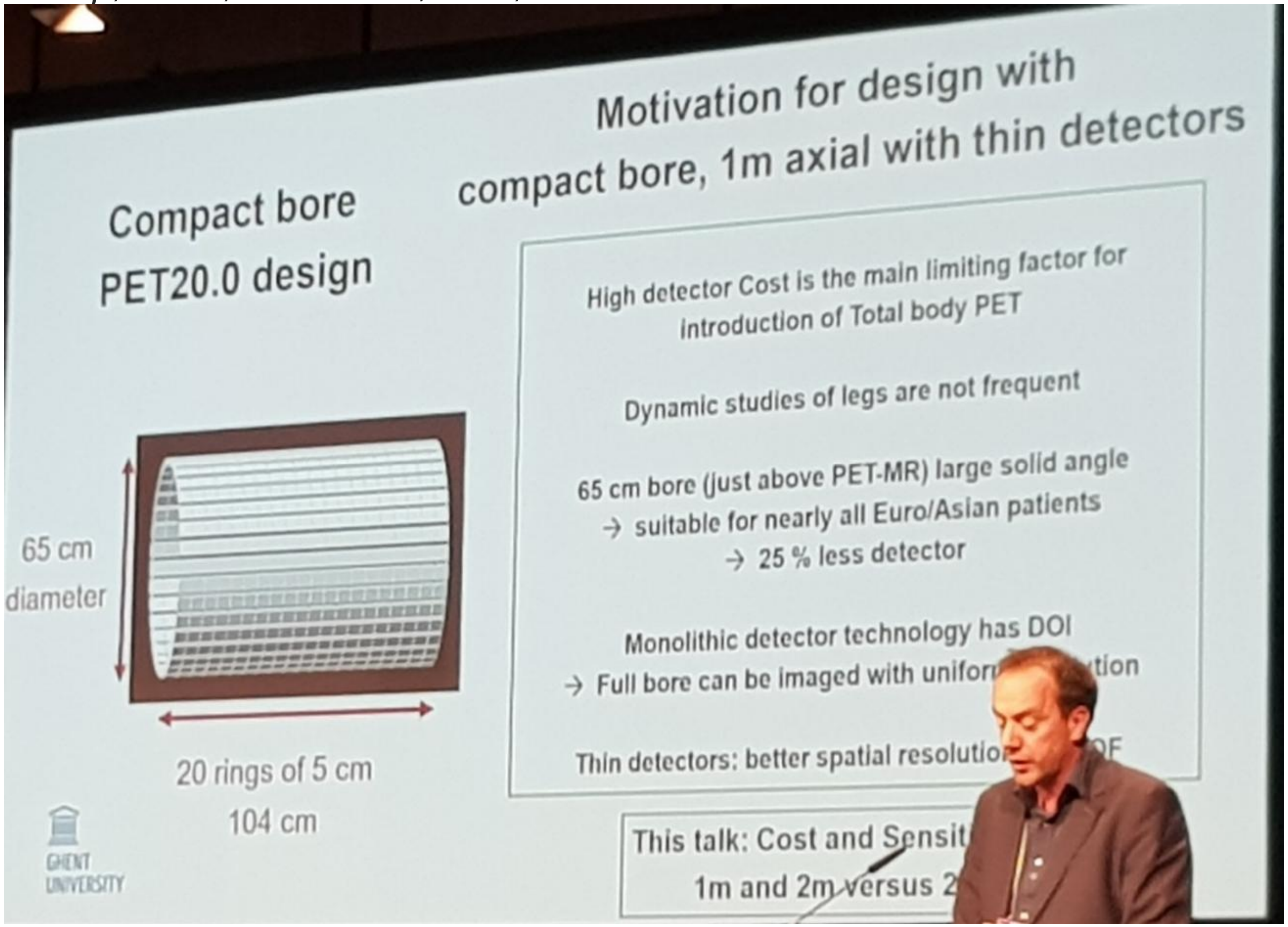

EANM 2017

Long Axial FOV – Total Body PET

- UC Davies
  - 2 m AxFOV with 25-50 x NEC high sensitivity
  - TOF and DOI essential

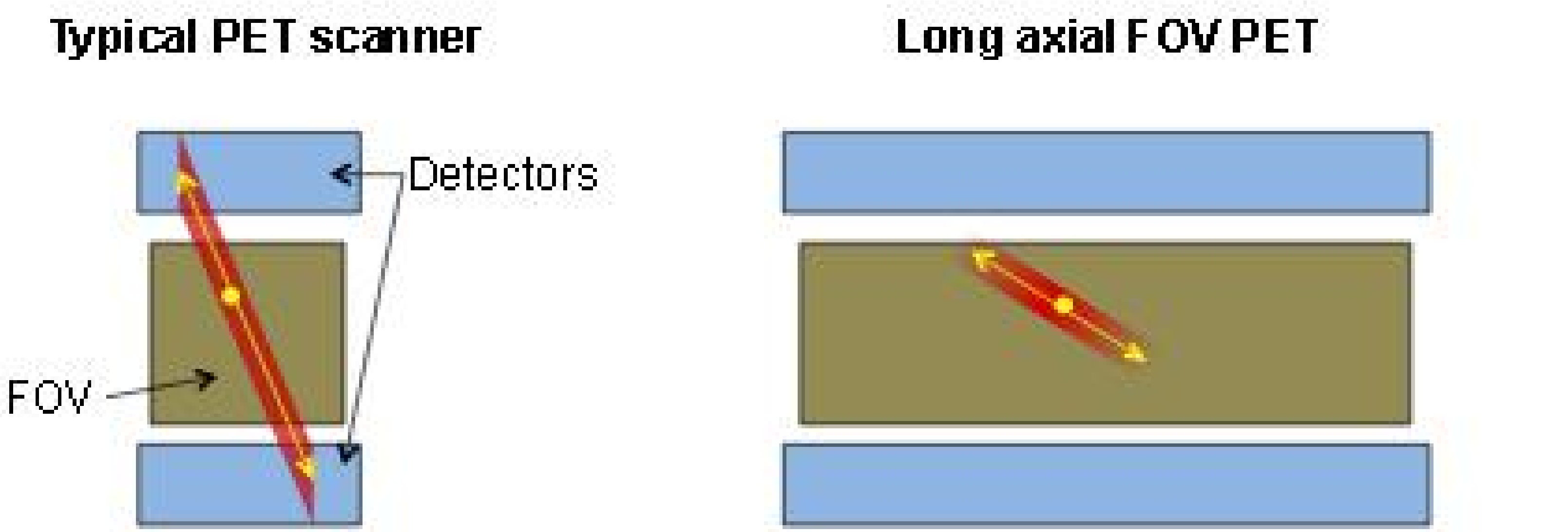

EXPLORER PROJECT

5 y NIH research award - $ 15.5 million

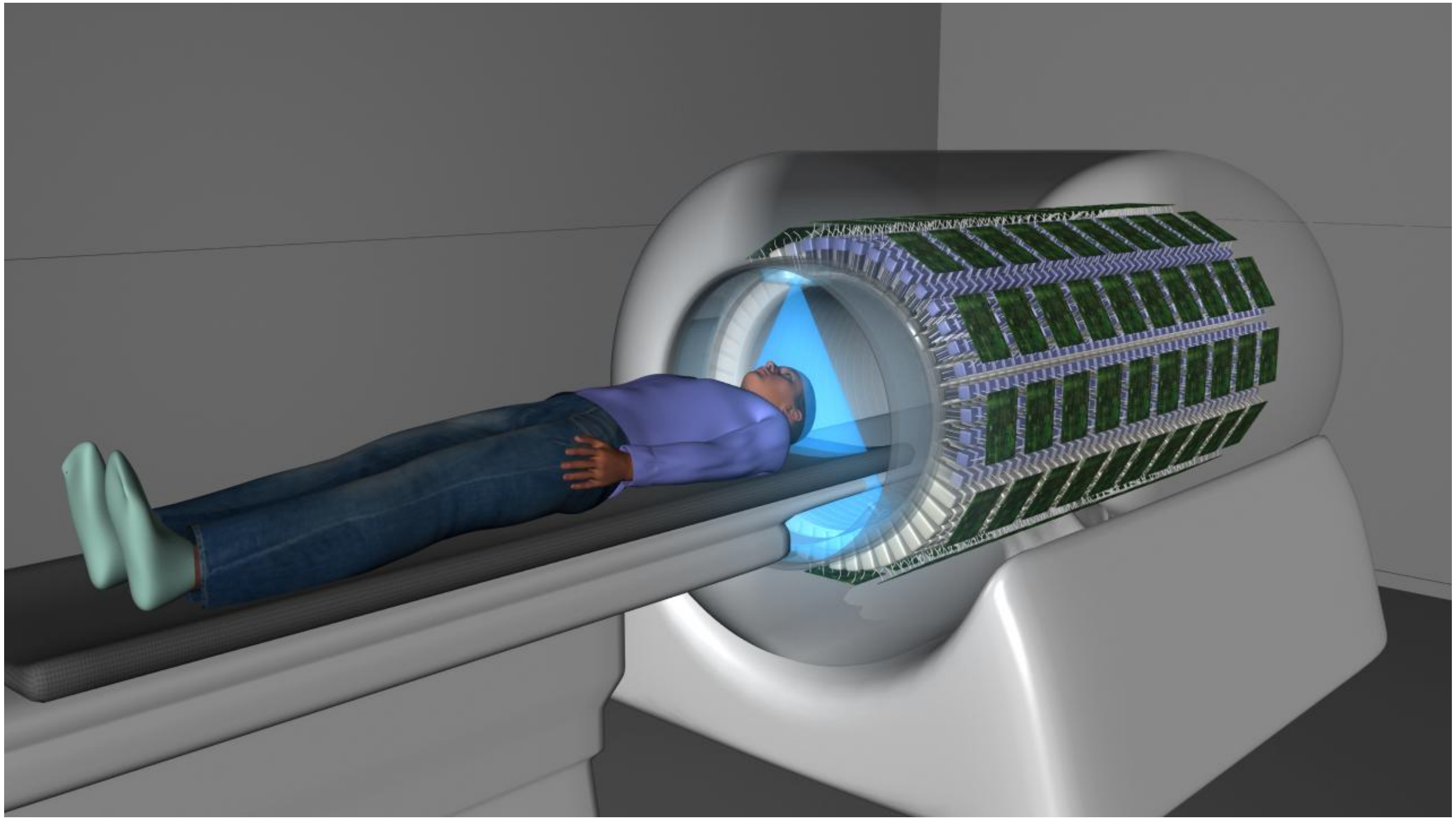

http://explorer.ucdavis.edu/

Total body PET – from mice to men

The first interactive, multidisciplinary conference focused on new technology and systems, fast, dynamic imaging and low dose applications of Total Body PET in animal science and medicine.

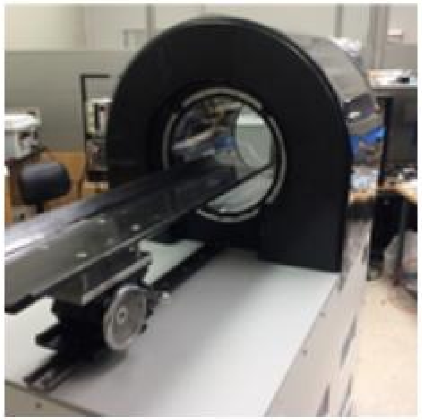


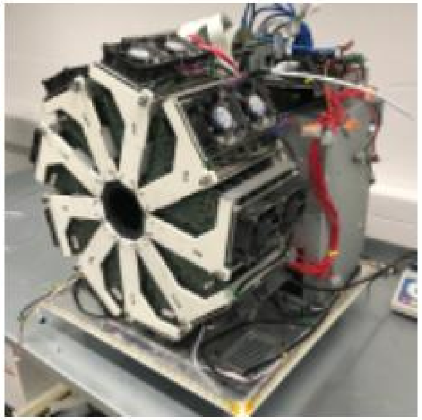

The Total Body PET conference 2018 is organized by Ghent University and the Ghent University Hospital. June 30 – July 2, 2018, Thagaste, Ghent (Belgium)

- Turku PET group
  - Juhani Knuuti – the driving force
  - Tuula Tolvanen – Phantoms
  - Mika Teräs – Project manager
  - Hidehiro Iida – Perfusion etc
  - Virva Saunavaara –PET/MR
  - Jarmo Teuho – Corrections
  - Mojtaba Jafari Tadi – Dual gating
  - Riku Klen – Motion correction
  - Jani Linden – reconstruction algorithms
  - + Many More

- Collaborators
  - Eero Lehtonen, Future Technologies, UTU
  - Kris Thielemans, Brian Hutton, UCL
  - Valentino Bettinardi, HSR Milan
  - Thomas Beyer, MUV, Vienna

- Master Research Agreements with TUH
  - GEHC
  - Philips

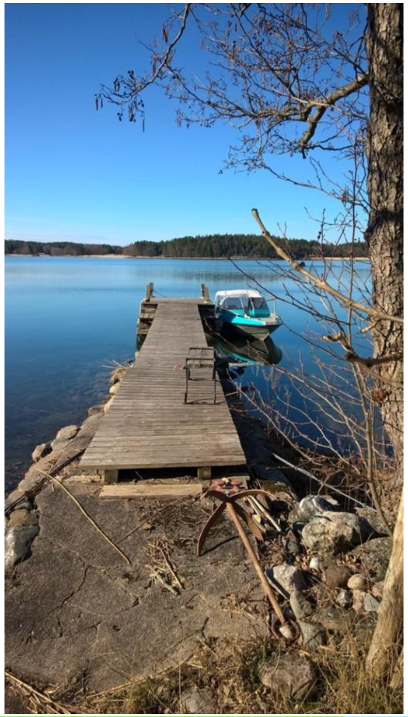

Thank you for your attention !

60°.51, 21°.35

Turku BioImaging

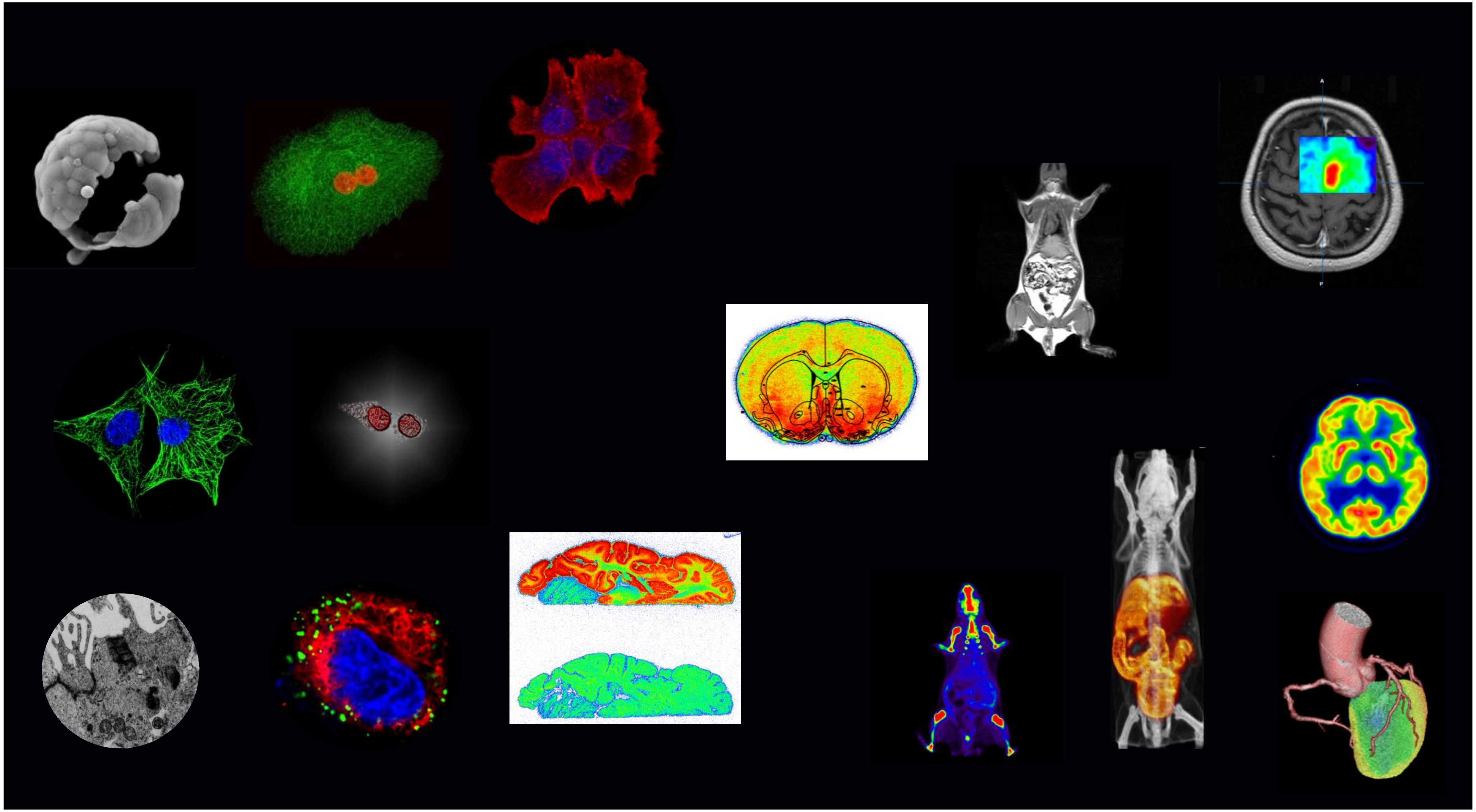

Nanoscopic

Cell

In vitro tissue

Ex vivo

In vivo non-clinical

Clinical